Spiekman et al. *Swiss Journal of Palaeontology* (2024) 143:10
https://doi.org/10.1186/s13358-024-00309-6

Swiss Journal of Palaeontology

RESEARCH ARTICLE

Open Access

A redescription of *Trachelosaurus fischeri* from the Buntsandstein (Middle Triassic) of Bernburg, Germany: the first European *Dinocephalosaurus*-like marine reptile and its systematic implications for long-necked early archosauromorphs

Stephan N. F. Spiekman[1*], Martín D. Ezcurra[2], Adam Rytel[3], Wei Wang[4], Eudald Mujal[1,5], Michael Buchwitz[6] and Rainer R. Schoch[1,7]

Abstract

Some of the earliest members of the archosaur-lineage (i.e., non-archosauriform archosauromorphs) are characterised by an extremely elongated neck. Recent fossil discoveries from the Guanling Formation (Middle Triassic) of southern China have revealed a dramatic increase in the known ecomorphological diversity of these extremely long-necked archosauromorphs, including the fully marine and viviparous *Dinocephalosaurus orientalis*. These recent discoveries merit a reinvestigation of enigmatic Triassic diapsid fossils from contemporaneous European deposits housed in historical collections. Here, we provide a redescription of *Trachelosaurus fischeri*, represented by a single, disarticulated specimen first described in 1918. Due to its unique morphology, which includes short, bifurcating cervical ribs, and a high presacral vertebral count, this taxon has been referred to either as a "protorosaurian" archosauromorph or a sauropterygian. Our revision clearly shows that *Trachelosaurus* represents the first unambiguous *Dinocephalosaurus*-like archosauromorph known from outside the Guanling Formation. Our finding has important systematic implications. Trachelosauridae Abel, 1919 represents the senior synonym for the recently identified Dinocephalosauridae Spiekman, Fraser and Scheyer, 2021. Based on our phylogenetic analyses, which employ two extensive datasets, we also corroborate previous findings that tanystropheids and trachelosaurids represent two families within a larger monophyletic group among non-crocopodan archosauromorphs, which is here named Tanysauria (clade nov.). Trachelosauridae is minimally composed of *Trachelosaurus fischeri*, *Dinocephalosaurus orientalis*, *Pectodens zhenyuensis*, and *Austronaga minuta*, but one of our analyses also found a probably taxonomically broader clade that may also include *Gracilicollum latens* and *Fuyuansaurus acutirostris*. *Trachelosaurus fischeri* considerably expands the known spatial and temporal range of Trachelosauridae to the earliest Anisian and the Central European Basin. Our findings add to the growing evidence for the presence of a diverse group of fully marine reptiles during the Middle Triassic

Editorial handling: Nicole Klein

*Correspondence:
Stephan N. F. Spiekman
stephanspiekman@gmail.com
Full list of author information is available at the end of the article

among Tanysauria. These trachelosaurids possess flipper-like limbs, high vertebral counts, and elongate necks, thus superficially resembling long-necked Jurassic and Cretaceous plesiosaurs in some regards.

Keywords Trachelosaurus, *Tanysauria*, Dinocephalosaurus, *Archosauromorpha*, *Middle Triassic*, *Buntsandstein*, *Osteology*, *Phylogeny*, *Marine reptiles*

Introduction

Non-archosaurian archosauromorphs represent the ancestral paraphyletic group of Archosauria, which is the clade that includes extant crocodylians and birds (Nesbitt, 2011). Stem-archosaurs originated in the late Permian and went extinct at the end of the Triassic (Ezcurra, 2016; Ezcurra & Butler, 2018; Ezcurra et al., 2014). They are not only fundamental to our understanding of archosaur origins, but also constitute a highly diverse group throughout the Triassic, particularly during the late Early-to-Middle Triassic, forming a major component of terrestrial vertebrate faunas in the aftermath of the end-Permian mass extinction (Foth et al., 2016; Spiekman et al., 2021b). Among the archosauromorphs most distantly related to crown archosaurs (i.e., "early diverging" or "basal" archosauromorphs) are enigmatic forms that are generally characterised by slender bodies and elongate necks. Historically, these taxa were referred to "Protorosauria", but recent phylogenetic studies suggest that they form a para- or polyphyletic grouping (Ezcurra, 2016; Pritchard et al., 2015), consisting among others of tanystropheids and a recently recognised family-level clade that includes the marine reptile *Dinocephalosaurus orientalis*, which has been named "Dinocephalosauridae" (Spiekman et al., 2021b, 2024). These long-necked archosauromorphs form a highly disparate group, including terrestrial, semi-aquatic, fully marine, and possibly gliding taxa (Dzik & Sulej, 2016; Spiekman et al., 2021b). Despite these recent findings, much remains unclear about their mode of life and phylogeny due to a combination of relatively incomplete and taphonomically compressed specimens and mosaic evolution, particularly of their cervical vertebral column (Spiekman et al., 2021b; Wang et al., 2023b).

Trachelosaurus fischeri is a highly enigmatic taxon that has previously been identified as a "protorosaur" (Broili & Fischer, 1918; Huene, 1944). It adds to the already complex evolution of early archosauromorph cervical morphology by possessing unique, stocky cervical ribs with a distally bifurcating shaft. The material attributed to *Trachelosaurus fischeri* (MLU.GeoS.1612, housed in the Geowissenschaftliche Sammlungen, Martin-Luther-Universität Halle-Wittenberg, Germany) is largely disarticulated and distributed over several associated slabs that derive from the Solling Formation (Middle Buntsandstein) of Bernburg an der Saale, Germany (Hauschke et al., 2005; Schoch, 2019; Fig. 1). MLU.GeoS.1612 was first acquired by Christian Gottfried Giebel of the Martin-Luther-Universität Halle-Wittenberg in the second half of the nineteenth century from O. Merkel (Broili & Fischer, 1918; Huene, 1902), owner of the quarry from which the specimens derived (now known as Merkel's Quarry; Fig. 1). The material was not studied until it came to the attention of Giebel's successor, Karl von Fritsch. Fritsch initially considered at least part of the material to belong to a sauropterygian, as is indicated by the presence of a label on MLU.GeoS.1612.D stating "*Conchiosaurus*?" (Broili & Fischer, 1918, p. 360; Fig. 2A). The genus name *Conchiosaurus* (type species *Conchiosaurus clavatus* Meyer, 1834, a small sauropterygian known from limited remains from the Muschelkalk of Braunschweig) is a junior synonym of *Nothosaurus* (International Commission on Zoological Nomenclature, 1998; Rieppel & Brinkman, 1996; Rieppel & Wild, 1996). Later, Huene (1902) mentioned that Fritsch considered the material to be attributable to a "proterosaurid" (i.e., a "protorosaur"). Huene (1902) also provided a brief, preliminary description of the material and agreed with the interpretation of Fritsch, in part based on a close similarity between one of the cervical vertebrae on the slabs and those of *Protorosaurus speneri*.

MLU.GeoS.1612 again fell out of interest for a considerable time after this, until it was rediscovered for a second time by Fritsch's successor Johannes Walther. Additional preparation was conducted and the material was entrusted to Ernst Fischer for study. Fischer was far progressed with his description when he died in battle in August 1914 during the First World War. The project was taken up and completed by Ferdinand Broili and, in a comprehensive monograph, the reptile remains on the slabs were attributed to a single individual of a new taxon, *Trachelosaurus fischeri* Broili, 1918. They reconstructed *Trachelosaurus* as a reptile with a total body length of approximately 150–170 cm, comprising a relatively small head, a very long and flexible neck consisting of 20–21 cervical vertebrae, a barrel-shaped torso, relatively short limbs, and a moderately long tail. It was inferred to be a terrestrial animal based on the shape of the ilium. In contrast to Fritsch and Huene (1902), Broili and Fischer (1918) did not think that *Trachelosaurus fischeri* represented a close relative of *Protorosaurus speneri*, with

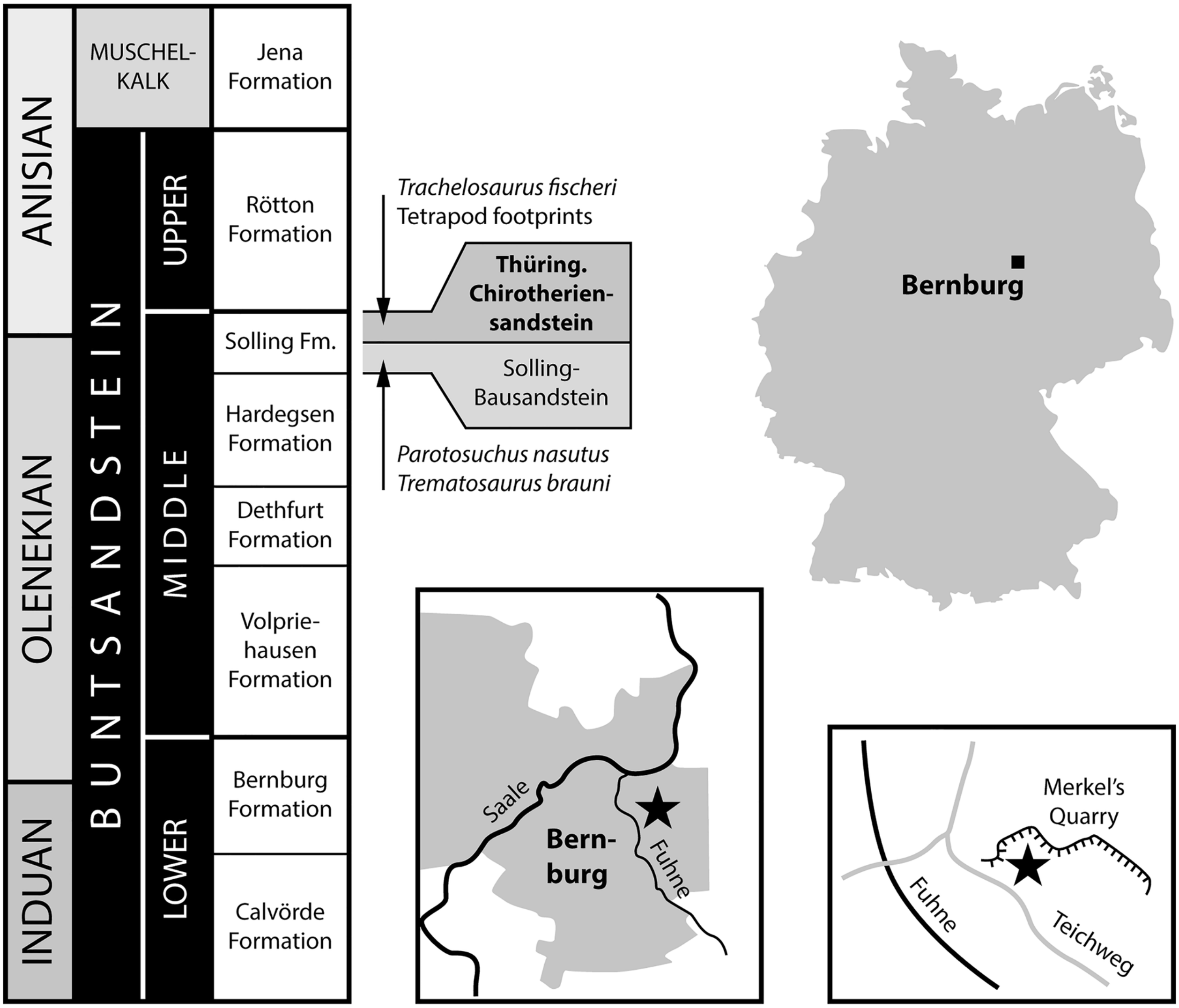

Fig. 1 Geographic and geological setting. Locality and stratigraphic context of Merkel's Quarry, where *Trachelosaurus fischeri* was found. Modified from Schoch (2019)

the most important argument being its high number of cervical vertebrae, which they considered more in correspondence with cervical counts of Triassic sauropterygians such as nothosaurs. Despite this, Broili and Fischer (1918) also pointed out several differences between *Trachelosaurus fischeri* and sauropterygians, such as the relative elongation of the cervical vertebrae, the fusion of the neurocentral suture of the vertebrae, and the more terrestrial configuration of the ilium. As such, they considered *Trachelosaurus fischeri* to represent a member of a separate and unique group within Sauropterygia, near the base of the clade, which was named Trachelosauria. This interpretation was also followed by later authors during this period (Arthaber, 1924; Nopcsa, 1923, 1928), who also assigned *Trachelosaurus fischeri* to its own family, Trachelosauridae (Abel, 1919).

Huene (1944) later provided a revision of *Trachelosaurus fischeri*. This was based on the figures and plates presented by Broili and Fischer (1918), since MLU. GeoS.1612 was stored away in Halle due to risk of air raids during the Second World War, and was thus not available for study. In contrast to Broili and Fischer (1918), Huene found that the cervical vertebrae did not belong to a single column of 20–21 consecutive vertebrae, but rather to two separate individuals, one preserving a series of nine cervical vertebrae, and five disarticulated cervical vertebrae belonging to another individual. Several other cervical vertebrae were reidentified as caudal vertebrae. Thus, the number of cervical vertebrae of

Trachelosaurus fischeri fell within the range known for "protorosaurs" at the time. Consequently, Huene (1944) maintained his earlier interpretation that *Trachelosaurus fischeri* was a "protorosaur", and later suggested that *Trachelosaurus fischeri* and many other "protorosaurs" fitted within Squamata (Huene, 1956).

Since Huene (1944), the material attributed to *Trachelosaurus fischeri* has not been studied in detail. Although it was incorporated in some early cladistic analyses and recovered among traditional "protorosaurs", it was found as highly unstable and omitted from most of the final results (Benton & Allen, 1997; Evans, 1988; Jalil, 1997; Rieppel et al., 2003). Due to a lack of information on this taxon, it was omitted from more recent phylogenetic studies (e.g., Ezcurra, 2016; Pritchard et al., 2015; Spiekman et al., 2021b), and its exact morphology, mode of life, and phylogenetic affinities remained unclear. Here, we aim to provide a detailed redescription of *Trachelosaurus fischeri*, including a formal diagnosis, and to assess its phylogenetic position based on two separate, up-to-date morphological character matrices, both focusing on archosauromorphs, which has important systematic implications for early (i.e., non-crocopodan) archosauromorphs.

Geological setting

Geographic and geological context

MLU.GeoS.1612 was collected at Merkel's Quarry, eastwards from Bernburg an der Saale (Saxony-Anhalt, Germany; Fig. 1). The rock exposure is around 90 m in width and is composed of sandstones from the Solling Formation. This quarry, which was active until the 1920s, has yielded numerous tetrapod remains, including hundreds of temnospondyl skulls (Schoch, 2018, 2019).

The Solling Formation forms the top of the Middle Buntsandstein (Hauschke et al., 2005; Fig. 1) and encompasses the Lower–Middle Triassic boundary (Bachmann et al., 2021). This formation is bounded by two unconformities and divided in two main intervals, the Solling-Bausandstein at the base and the Chirotheriensandstein at the top. The lower interval is relatively coarse-grained, and some levels may also contain (micro-) conglomerates. It was deposited in the proximal part of the basin, infilling, and overlying older fluviatile channels (Puff & Radzinski, 2013). The temnospondyl remains come from this lower interval (Schoch, 2018, 2019). The upper interval consists mainly of sandstones. Hauschke et al. (2005) differentiated three major lithofacies (Sandy, Silty, and Muddy Facies). These authors identified patterns of polymodal palaeocurrent, including small- to large-scale herringbone cross bedding, mud-drapes, reactivation surfaces, graded and lenticular bedding, mud-cracks, and mottling. All these features indicate a coastal setting under tidal (i.e., marine) influence (Hauschke et al., 2005). As its name indicates, the Chirotheriensandstein is rich in chirotheriid footprints, as well as other ichnotaxa, such as *Capitosauroides bernburgensis* (Haubold, 1971; Klein, 2021).

Sedimentology of the specimen

The seven fitting slabs that contain the fossils (Fig. 2B) are composed of cross bedded fine-grained sandstone (Fig. 2C). Two different depositional intervals can be distinguished in the cross sections of the slabs (Fig. 2C, D): (1) a tabular layer ~ 1.3 cm thick that contains the bones and footprints in convex hyporelief (which indicate that this is the stratigraphically lowest interval of the slabs), and (2) a trough cross-laminated layer ~ 5.0 cm thick. The boundary between the two intervals is well marked in several sections of the slabs (Fig. 2D), denoting changes in the water flow regime. The top surface of the slabs (i.e., opposite to the surface with bones and footprints) displays ramified structures (Fig. 2E) that could potentially be syneresis cracks (structures similar to desiccation cracks that form under water: Pratt, 1998) or invertebrate burrows. The trough cross-lamination in the upper interval presents two main opposing directions (herringbone-like; Fig. 2C), thus indicating a main bidirectional water current. In some other sections of the slabs, other subordinate directions of the cross-lamination are observed. Regarding the lower interval, the surface exposing the bones and footprints is relatively flat, though it has a rugose aspect given by small round structures in convex hyporelief that could correspond to raindrop imprints and/or to wrinkle structures due to desiccation of microbial mats (Fig. 2F). A square structure of 0.5 × 0.5 cm (Fig. 2G), also preserved in convex hyporelief, is present on slab (d). This structure corresponds to a mould of a salt (likely halite) crystal that typically forms because of precipitation of salt minerals during water evaporation. Tetrapod footprints (asterisks in Fig. 2B) are very shallowly impressed but relatively well defined (Fig. 2H). Considering their relatively small size and the lithology and sedimentary structures of the slab, the footprints were probably formed in a relatively firm substrate and covered soon after their impression, together with the skeletal remains. All in all, the set of sedimentological features indicates a saline environment with bidirectional (or multidirectional) water flows, characteristic of tidal flats that undergo periods of evaporation and desiccation (likely from the intertidal zone). This palaeoenvironmental interpretation is in accordance with that of the upper part of the Solling Formation (Chirotheriensandstein) by Hauschke et al. (2005).

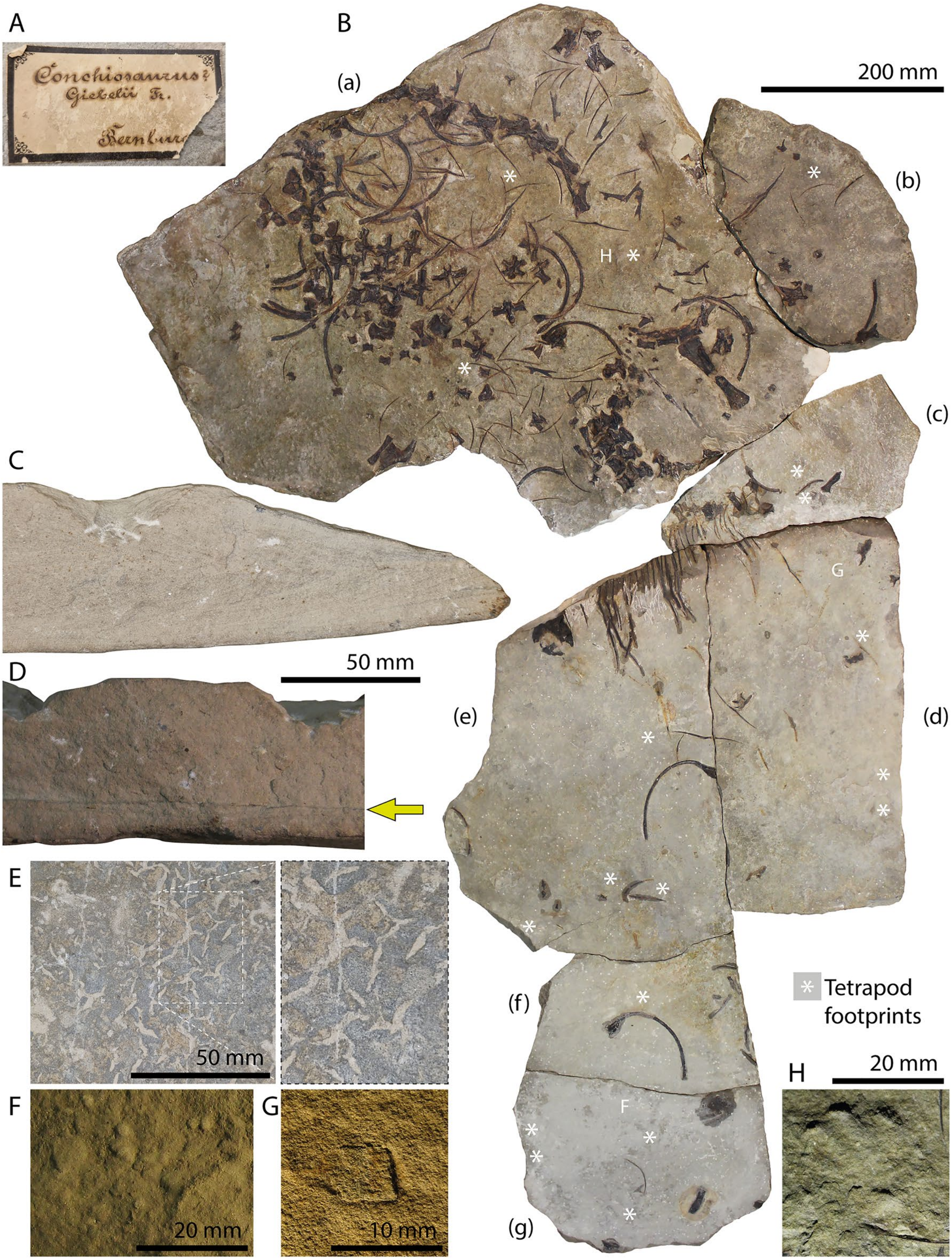

Fig. 2 Overview of MLU.GeoS.1612 and its sedimentary features. **A**, Historical label on the slab. **B**, Overview of MLU.GeoS.1612, the holotype of *Trachelosaurus fischeri*; the bracketed lower case letters correspond to the different slabs of which the specimen is composed. The asterisks (*) indicate tetrapod footprints preserved on the slabs. **C**–**D** Slab in cross-section, with trough cross-lamination (**C**) and the two intervals with an arrow pointing at their boundary (**D**). **E** Sinuous and ramified structures on the top surface (opposite to the surface preserving bones and footprints), including a close-up on the right. **F** Round structures. **G** Squared structure. **H** Tetrapod footprint (left manus) previously mentioned in Broili and Fischer (1918). Structures in **F**–**H** are in convex hyporelief, and their location is marked with matching upper case letters on the overview of the specimen in B

Materials and methods

Phylogenetic analyses

The phylogenetic position of *Trachelosaurus fischeri* was tested by incorporating it into two separate morphological phylogenetic matrices focused on non-archosaurian archosauromorph interrelationships. The first matrix focusses specifically on non-crocopodan archosauromorphs, and was first presented in Spiekman et al. (2021b). It has subsequently been modified and updated in Wang et al., (2023a, 2023b), Lu and Liu (2023), and Spiekman et al., (2024). In the current contribution, we have added *Trachelosaurus fischeri*, modified several scorings for other taxa, and edited some character definitions (see Additional file 1). The second matrix is that of the Complete Archosauromorph Tree Project (CoArTreeP) and focuses more broadly on Permian–Triassic archosauromorph interrelationships. It was first introduced by Ezcurra (2016) and it has subsequently been modified more than 20 times. The matrix used here merges the data matrices of Ezcurra et al. (2023), Paes-Neto et al. (2023), and Müller et al. (2023), which are all parallel ramifications of the genealogy of the CoArTreeP phylogenetic matrix. In addition, here we have modified some scorings and characters with respect to previous versions of the matrix (see Additional file 2).

The new iteration of the Spiekman et al. (2021b) matrix was analysed using TNT 1.6 (Goloboff & Morales, 2023). Three operational taxonomic units (OTUs) were deactivated a priori: *Czatkowiella harae*, *Tanystropheus "conspicuus"*, and *"Tanystropheus antiquus"* (for justification, see Spiekman et al., 2021b, p. 49). The following characters were treated as ordered, because they represent nested sets of homologies: 1, 2, 4, 5, 7, 9, 13, 35, 43, 62, 73, 77, 78, 83, 84, 88, 89, 110, 114, 118, 128, 136, 140, 144, 153, 158, 159, 162, 178, 185, 187, 194, 195, 200, 205, 209, 219, 220, 224, 230, 232, 242, 248, 251, 258, 259, 267, 276, 292, 294, 297, 298, 299, and 305. Tree searches under equal character weighting were performed using a Traditional Search with 1,000 Wagner trees replications, random addition sequence, and TBR branch swapping holding ten trees per replicate. Values of Bremer and Bootstrap support (GC = groups recovered versus groups contradicted) were calculated, the latter through a Traditional search with 1,000 iterations. Homoplasy indices were calculated with a script that does not take into account a priori deactivated terminals (STATSb.run; see Electronic Supplementary Material of Spiekman et al., 2021a). Unstable OTUs were identified and removed from the strict consensus tree (SCT) a posteriori using the iterPCR protocol of TNT (Pol & Escapa, 2009) to recover a more completely resolved reduced strict consensus tree (RSCT).

The CoArTreeP matrix is a considerably larger dataset and, thus, we used a different protocol for its analysis. The dataset was analysed using TNT 1.6 (Goloboff & Morales, 2023) with parallelisation under the Parallel Virtual Machine system (Morales & Goloboff, 2023). The analyses were conducted in one of the clusters (96 cores) of the Centro de Computación de Alto Desempeño of the Universidad Nacional de Córdoba (Argentina) using a custom script written here for TNT (treeSearches_protocol_cluster.run) to implement parallel computing during tree searches and resampling analyses (Additional file 2). Here, we modified six characters, modified several scorings, and added five non-crocopodan archosauromorph species (*Sclerostropheus fossai*, *Ozimek volans*, *Gracillicolum latens*, *Austronaga minuta*, and *Luxisaurus terrestris*; Wild, 1980; Dzik & Sulej, 2016; Spiekman & Scheyer, 2019; Lu & Liu, 2023; Wang et al., 2023a, 2023b; see Additional file 2). We deactivated the following 41 OTUs before the tree searches, because they were scored only for the purpose of morphological disparity analyses, are not diagnostic at a species level, or are combinations between other OTUs: ISIR 1132, *"Protanystropheus antiquus"* (= *"Tanystropheus antiquus"*), *"Tanystropheus haasi"*, *Malerisaurus* all NA, *Arctosaurus osborni*, CRILAR-Pv 461, CRILAR-Pv 462, CRILAR-Pv 497, Chanares rhynchosaur, PVSJ 2728, *Eorasaurus olsoni*, *Archosaurus rossicus* holotype, *Blomosuchus georgii* holotype, *Samsarasuchus pamelae* expanded, *Kalisuchus rewanensis* combined, UFSM 11444, UFSM 11394, UNIPAMPA 271, UNIPAMPA 684, *Vonhuenia friedrichi* holotype, *Chasmatosuchus rossicus* holotype, *Jaikosuchus* Ochev hypodigm, *Chasmatosuchus vjushkovi*, *Koilamasuchus gonzalezdiazi*, CRILAR-Pv 499, *Shansisuchus kuyeheensis*, *Uralosaurus* combined, *Osmolskina czatkoviensis*, *Osmolskina* complete, *Triopticus primus*, Otter Sandstone archosaur, *Dagasuchus santacruzensis*, *Ctenosauriscus koeneni*, *Hypselorhachis mirabilis*, Waldhaus poposauroid, *Jaikosuchus* + *Vytshegdosuchus*, *Bystrowisuchus flerovi*, *Bromsgroveia walkeri*, *Lutungutali sitwensis*, *Nyasasaurus parringtoni*, and *Ignotosaurus fragilis*. Characters 9 and 119 were deactivated before any analysis (following Ezcurra et al., 2017, and Butler et al., 2019). The final modified data set is composed of 238 active terminals and 907 active characters (see Additional file 2). The following characters were treated as ordered following the same arguments as outlined above: 1, 2, 7, 10, 17, 19–21, 28, 29, 34, 36, 40, 42, 46, 50, 54, 66, 71, 74–76, 100, 122, 127, 146, 153, 156, 157, 171, 176, 177, 187, 202, 221, 227, 263, 266, 278, 279, 283, 311, 324, 327, 331, 337, 342, 345, 350–352, 354, 361, 365, 368, 370, 377, 379, 386, 387, 398, 410, 414, 416, 424, 425, 430, 435, 446, 448, 454, 455, 458, 460, 463, 464, 470, 472, 478, 482, 483, 485, 489, 490, 502, 504, 510, 516, 520, 521, 529, 537, 546, 552, 556, 557, 567, 569, 571, 574, 581, 582, 588, 636, 648, 652, 662, 701, 731, 735, 737, 738, 743, 749, 766, 784, 803, 809, 810, 816, 850, 851, 875, 885, 888, 894, 898, 900, and 909.

The analyses of the CoArTreeP matrix were conducted under implied weighting with concavity constants (k) of k = 19–24 (i.e., a total of six analyses). This decision of weighting against homoplasy follows the results and recommendation of Ezcurra (2023), in which implied weighting outperformed the results under equal weighting, and k values between 19 and 24 showed the best performances throughout the genealogy of this phylogenetic data matrix. The tree searches followed a slightly modified version of the protocol used by Pei et al. (2020). New technology search algorithms (initially using 5 random addition sequence Wagner trees followed by tree bisection reconnection, sectorial searches, and 5 cycles of tree-drifting, followed by tree fusing) were used to calculate a consensus when trees of optimal score were repeatedly found (collapsing zero-length branches). The search was stopped only when the consensus became stable to new hits. Thus, the optimal score was found independently as many times as needed to obtain a stable consensus; this validation procedure was performed one time in 20 cores of the cluster (i.e., 20 stable consensus trees). This consensus stabilisation procedure can produce an accurate consensus without finding all equally possible most parsimonious trees (MPTs), which in large palaeontological datasets tend to be a number considerably larger than those that common computers can store, and considerably reduce computation time (Goloboff, 1999). As Pei et al. (2020) highlighted: “the trees found by the routines (…) are a representative sample of all possible MPTs (instead of all the trees), and their consensus is expected to be identical to the consensus of all possible MPTs for the dataset.” The ‘prunnelsen’ command was used to detect topologically unstable terminals among the most parsimonious trees of each analysis.

Homoplasy indices for each analysis under different k values were calculated with STATSb.run. Group supports were quantified using no-zero weight symmetric resampling analyses, because implied character weighting was used here and the resampling should increase or decrease the weight of the characters with the same probability to avoid distortions produced by different implied weights (Goloboff et al., 2003). The prior weights were doubled or halved with the same probability of 25%. Tree searches in the resampled matrices were conducted using sectorial searches, drifting, ratchet, and tree fusing, until one hit of an optimal tree was achieved in each of a total of 10,000 pseudo-replicates. The pseudo-replicates were distributed among the 96 cores of the cluster to reduce computational time, using a modified version of the psample.run script written by Morales and Goloboff (2023). Pei et al. (2020) noted that no-zero weight symmetric frequencies cannot be interpreted in the same way as standard bootstrap frequencies, but should be interpreted as a measure of the degree to which the characters in the dataset present conflict in regard to the monophyly of the group. Both absolute frequencies and frequency differences (i.e., GC) were reported on the strict consensus tree of each analysis.

Finally, a global SCT was generated from all the MPTs found in the different analyses under implied weighting with the different k values. Similarly, absolute and frequency difference resampling frequencies were calculated from all the resampling trees recovered in the different analyses. The ‘prunnelsen’ command was used again to detect topologically unstable terminals among all these MPTs.

Results

Systematic palaeontology

Diapsida Osborn, 1903.

Archosauromorpha von Huene, 1946.

Tanysauria clade nov.

Etymology. ‘*Tany*’, meaning long (Greek), and ‘*sauros*’, meaning lizard, referring to the elongated necks and in some cases also bodies of the taxa belonging to this clade.

Phylocode registration number. Tanysauria is identified in the international clade names repository as registration number 1027.

Phylogenetic definition. All taxa more closely related to *Tanystropheus longobardicus* (Bassani, 1886), *Dinocephalosaurus orientalis* Li, 2003, and *Trachelosaurus fischeri* Broili, 1918 than to *Protorosaurus speneri* von Meyer, 1832, *Prolacerta broomi* Parrington, 1935, *Mesosuchus browni* Watson, 1912, *Azendohsaurus madagaskarensis* Flynn et al., 2010, or *Proterosuchus fergusi* Broom, 1903. This is a maximum clade definition.

Reference phylogeny. Phylogenetic hypotheses recovered in this paper.

Composition. The composition is based on our reference phylogenies. Tanysauria includes the following nominal species: *Tanystropheus longobardicus*, *Tanystropheus hydroides*, *Tanytrachelos ahynis*, *Ozimek volans*, *Sclerostropheus fossai*, *Raibliania calligarisi*, *Langobardisaurus pandolfii*, *Amotosaurus rotfeldensis*, *Macrocnemus bassanii*, *Macrocnemus fuyuanensis*, *Macrocnemus obristi*, *Luxisaurus terrestris*, *Augustaburiana vatagini*, *Dinocephalosaurus orientalis*, *Gracilicollum latens*, *Trachelosaurus fischeri*, *Fuyuansaurus acutirostris*, *Austronaga minuta*, *Pectodens zhenyuensis*, and ambiguously *Jesairosaurus lehmani* and *Elessaurus gondwanoccidens*.

Diagnosis. Tanysauria is a clade that is defined among other archosauromorphs by possessing the following unique combination of character states: premaxilla with five or more tooth positions (absent in *Langobardisaurus pandolfii*); postfrontal medial margin lateral to parietal; parietal extending over interorbital region (absent in *Tanytrachelos ahynis*); interclavicle anterior margin with a median notch (absent in taxa that lack an ossified interclavicle); and humerus with moderate medial development of the entepicondyle, being poorly projected from the level of the shaft (absent in *Ozimek volans*). In addition, the following character states are absent in *Jesairosaurus lehmani* and are synapomorphies of Tanysauria if this species is not recovered at the base of the clade or are apomorphies of a more restricted Trachelosauridae + Tanystropheidae clade if *Jesairosaurus lehmani* is positioned at the base of Tanysauria: axis with an anterodorsally expanded neural spine; anterior to middle postaxial–cervical vertebrae strongly elongated, with a ratio between centrum length versus height of anterior articular surface greater than 2.92; scapula with a semi-circular outline in lateral view formed by a scapular blade that has a convex anterior margin and a predominantly posterior orientation; and scapula and coracoid that are unfused with each other in non-early juvenile individuals (absent in *Ozimek volans*).

Trachelosauridae Abel, 1919[1] (= Dinocephalosauridae Spiekman, Fraser and Scheyer, 2021)

1919	Trachelosauridae	Abel, p. 481–483
1923	Trachelosauridae	Nopcsa, p. 124
1928	Trachelosauridae	Nopcsa, p. 172
1935	Trachelosauridae	Kuhn, p. 28
1960	Trachelosauridae	Kuhn, p. 35
1961a	Trachelosauridae	Kuhn, p. 40
1963	Trachelosauridae	Kuhn, p. 6
1971	Trachelosauridae	Kuhn, p. 12
2021	Dinocephalosauridae	Spiekman et al., throughout text
2022	Dinocephalosauridae	Ezcurra & Sues, throughout text
2023	Dinocephalosauridae	Lu & Liu, throughout text
2023	Dinocephalosauridae	Sobral, p. 411; Fig. 17
2023b	Dinocephalosauridae	Wang et al., throughout text
2023a	Dinocephalosauridae	Wang et al., throughout text
2024	Dinocephalosauridae	Spiekman et al., throughout text

Phylocode registration number. Trachelosauridae is identified in the international clade names repository as registration number 1028.

Phylogenetic definition. The definition of Trachelosauridae is modified from the definition for Dinocephalosauridae (Spiekman et al., 2021b) as follows: the most inclusive clade containing *Trachelosaurus fischeri* Broili, 1918 and *Dinocephalosaurus orientalis* Li, 2003 but not *Tanystropheus longobardicus* (Bassani, 1886), *Macrocnemus bassanii* Nopcsa, 1931, *Protorosaurus speneri* von Meyer, 1832, or *Prolacerta broomi* Parrington, 1935. This is a maximum clade definition.

Reference phylogeny. Phylogenetic hypotheses recovered in this paper.

Composition. The composition is based on our reference phylogenies. Trachelosauridae includes the following nominal species: *Dinocephalosaurus orientalis*, *Trachelosaurus fischeri*, *Austronaga minuta*, *Pectodens zhenyuensis*, and ambiguously *Gracilicollum latens*, and *Fuyuansaurus acutirostris*.

Diagnosis. Trachelosauridae is a clade that is defined among other archosauromorphs by possessing the following unique combination of character states: external naris positioned far from the anterior end of the premaxilla, resulting in an anteroposteriorly deep base of the prenarial process; jugal without posterior process; cervical column composed of ten or more vertebrae (also present in some deeply nested tanystropheids); axis with postzygapophysis confluent with and not protruding posteriorly from the base of the neural spine in lateral view (also present in *Tanystropheus* spp. and *Amotosaurus rotfeldensis*); mid-dorsal vertebrae with very wide and 'wing-like' transverse processes; presence of holocephalous anterior dorsal ribs (also present in some tanystropheids); metatarsal V without a hook-shaped proximal end.

Trachelosaurus Broili & Fischer, 1918[2]

Trachelosaurus fischeri Broili, 1918[3]

1902	"*Protorosaurus*-ähnliches Reptil "	v. Huene, p 8–10; Fig. 4
1917	*Trachelosaurus Fischeri**	Berliner & Pütter, p. 767 *authorship given to Broili & Fischer

---

[1] Broili & Fischer, 1918 only used "Trachelosauria" as a higher rank taxon including *Trachelosaurus* (*contra* Kuhn, 1961a, 1963). The first use and authorship of the family name comes from Abel (1919), following Kuhn (1971).

[2] While the original description was predominantly cited as if published in 1917, it was contained within a journal issue printed in 1918.

[3] While the genus name could have been erected by either of the authors, the species name was given by F. Broili to commemorate E. Fischer, who died in 1914.

1918	*Trachelosaurus Fischeri*	Broili & Fischer, throughout text; Figs. 1–7, 15; plates 31–32
1919	*Trachelosaurus Fischeri*	Abel, p. 482–483
1920	*Trachelosaurus Fischeri*	Abel, p. 375
1921	*Trachelosaurus*	Edinger, p. 204
1922	*Trachelosaurus Fischeri*	Cossmann, p. 91
1923	*Trachelosaurus*	Nopcsa, p. 68
1924	*Trachelosaurus*	von Arthaber, p. 442
1927	*Trachelosaurus Fischeri*	Weigelt, p. 54, 118 (in the 1989 edition)
1928	*Trachelosaurus*	Nopcsa, p. 172
1928	*Trachelosaurus Fischeri*	Schmidt, p. 393; Fig. 1104
1932	*Trachelosaurus*	v. Zittel, p. 285
1933	*Trachelosaurus*	Gadow, p. 329
1935	*Trachelosaurus fischeri*	Kuhn, p. 28
1944	*Trachelosaurus fischeri*	v. Huene, throughout text
1948	*Trachelosaurus*	v. Huene, p. 102
1951	*Trachelosaurus*	Watson, p. 169
1952	*Trachelosaurus Fischeri*	Lang & v. Huene, p. 15
1954	*Trachelosaurus*	v. Huene, p. 229; Fig. 2d
1955	*Trachelosaurus*	Vaughn, p. 435–436, 448
1955	*Trachelosaurus*	Peyer & Kuhn-Schnyder, p. 598
1956	*Trachelosaurus*	v. Huene, p. 648, 683
1956	*Trachelosaurus*	Romer, p. 432, 657; Figs. 122L, 131D, 139O, 140X
1957	*Trachelosaurus*	Watson, Fig. 23
1961b	*Trachelosaurus*	Kuhn, p. 5
1963	*Trachelosaurus fischeri*	Kuhn, p. 3, 5–7
1967	*Trachelosaurus fischeri*	Appleby et al., p. 704
1969	*Trachelosaurus*	Carroll, p. 166
1971	*Trachelosaurus fischeri*	Kuhn, p. 12; Figs. 20a/1, 41b/8
1973	*Trachelosaurus*	Wild, p. 28
1975	*Trachelosaurus fischeri*	Kuhn, p. 8; Fig. 3
1982	*Trachelosaurus fischeri*	Mader, Table 2
1988	*Trachelosaurus*	Carroll, p. 619
1988	*Trachelosaurus*	Evans, p. 227–228
1994	*Trachelosaurus*	Renesto, p. 286
1997	*Trachelosaurus fischeri*	Benton & Allen, Table 1; text-Fig. 16
1997	*Trachelosaurus*	Jalil, throughout text
1999	*Trachelosaurus*	Borsuk-Białynicka et al., p. 182; Table 1
2000	*Trachelosaurus fischeri*	Rieppel, p. 110
2003	*Trachelosaurus*	Rieppel et al., throughout text
2008	*Trachelosaurus*	Hone & Benton, throughout text
2009	*Trachelosaurus*	Gottmann-Quesada & Sander, throughout text
2015	*Trachelosaurus fischeri*	Hauschke & Mertmann, p. 344
2016	*Trachelosaurus*	Ezcurra, p. 311
2018	*Trachelosaurus*	Hauschke, p. 286
2018	*Trachelosaurus fischeri*	Schoch, p. 108, 111
2019	*Trachelosaurus fischeri*	Schoch, p. 58
2021	*Trachelosaurus fischeri*	Hauschke et al., p. 333, 388
2021	*Trachelosaurus fischeri*	Spiekman et al., throughout text
2022	*Trachelosaurus fischeri*	Ezcurra et al., p. 5

Holotype. MLU.GeoS.1612, a partially disarticulated skeleton comprising a few isolated skull remains, including a right premaxilla, much of the presacral vertebral column, two sacral vertebrae, several caudal vertebrae, an extensive gastral basket, a right ilium, right? pubis, left? femur, and at least one probable metatarsal.

Diagnosis. A tanysaurian archosauromorph that is defined by the following combination of features (autapomorphies among Triassic archosauromorphs indicated by an asterisk): elongate vertebral column that consists of at least 21 cervical and 27 dorsal vertebrae; neural spines on both the cervical and dorsal vertebrae that are transversely expanded at their distal ends with strongly developed rugosities*; cervical ribs with bifurcating shafts that are short, not or barely extending beyond the length of its corresponding vertebra*; anterior to mid-dorsal vertebrae with very wide, 'wing-like' transverse processes; a barrel-shaped torso formed by widely rounded, almost uniformly holocephalous dorsal ribs; an ilium without a preacetabular process; and a stocky femur without a curved shaft.

Horizon. The type and only specimen of *Trachelosaurus fischeri* was found in a platy sandstone unit within the Chirotheriensandstein, upper part of the Solling Formation (topmost Middle Buntsandstein, probably of earliest Anisian age, see Schoch, 2019; Bachmann et al., 2021).

Locality. Merkel's quarry, Bernburg an der Saale, Saxony-Anhalt, central Germany.

Ontogenetic assessment. *Trachelosaurus fischeri* is currently known from a single specimen, MLU.GeoS.1612, comprising one individual (see below). In both the anteriormost cervical vertebra and mid-dorsal vertebrae, the neural arches and centra are unfused or disarticulated. Furthermore, the proximal and distal ends of the femur are poorly ossified. These features are often indicative of skeletal immaturity in diapsids (Griffin et al., 2021). However, they can also represent typical paedomorphic traits related to aquatic adaptations seen in skeletally mature marine reptiles, including *Dinocephalosaurus orientalis* (Griffin et al., 2021; Rieppel, 1989; Spiekman et al., 2024). Considering the presence of several features indicative of an aquatic lifestyle in *Trachelosaurus fischeri* (high presacral vertebral count, straight femur, and absence of preacetabular process of the ilium), and its close affinities to the marine *Dinocephalosaurus orientalis* (see below), the latter interpretation is very likely. Therefore, these features are not reliable indicators of relative ontogenetic age for this individual. The presence of strongly rugose neural spines on the presacral vertebrae could represent some indication of maturity, but this cannot be stated confidently.

Remarks. The most recent definition of Tanystropheidae Camp, 1945 was formulated by Dilkes (1998, page 529): "the most recent common ancestor of *Macrocnemus*, *Tanystropheus*, and *Langobardisaurus* and all of its descendants". Considering the discovery of many new tanystropheid taxa in recent years, as well as the results of our phylogenetic analyses and the novel definitions of Tanysauria clade nov. and Trachelosauridae Abel, 1919, we propose a revised definition for Tanystropheidae that is stem-based: the most inclusive clade containing *Tanystropheus longobardicus* (Bassani, 1886) but not *Trachelosaurus fischeri* Broili, 1918, *Dinocephalosaurus orientalis* Li, 2003, *Protorosaurus speneri* von Meyer, 1832, or *Prolacerta broomi* Parrington, 1935. This is a maximum clade definition.

Phylocode registration number. Tanystropheidae is identified in the international clade names repository as registration number 1040.

Description

MLU.GeoS.1612 consists of seven slabs that can be fitted together to form a single block (Fig. 2B). The majority of the remains of *Trachelosaurus fischeri*, including virtually all pre-caudal axial elements, are closely associated in MLU.GeoS.1612.A-B (Fig. 3). Additional remains, including cranial elements and a partial gastral basket, are scattered across MLU.GeoS.1612.C-G (Fig. 4). The slabs additionally preserve indeterminate remains of actinopterygian fishes, as well as several footprints resembling *Capitosauroides bernburgensis* and a tetrapod ichnotaxon possibly produced by therapsid trackmakers that was described from an unknown locality in the same area (Buchwitz et al., 2020; Haubold, 1971). The discovery of several tetrapod footprints while examining the slabs (in addition to those previously reported by Broili & Fischer, 1918) requires a more detailed description and analysis that are outside the scope of the present work (Fig. 2B).

Skull

Premaxilla. A right premaxilla is exposed in lateral view on MLU.GeoS.1612.D (Figs. 4, 5A). It preserves two teeth in situ, of which the posterior one is larger. The teeth are elongate and incipiently recurved, resembling the dentition of the premaxilla in *Tanystropheus* spp. (excluding *"Tanystropheus antiquus"*, here and throughout the text), *Austronaga minuta*, *Dinocephalosaurus orientalis*, and *Gracilicollum latens* (Wang et al., 2023a, 2023b). The teeth lack serrations, as in other tanysaurians (Ezcurra, 2016; Spiekman et al., 2021b). Their enamel surface is poorly preserved and the apical half of the larger tooth is broken, but the teeth appear to not be striated (Fig. 5B), in contrast to the striated crowns of *Tanystropheus* spp., *Dinocephalosaurus orientalis*, and *Gracilicollum latens* (Wang et al., 2023b). However, striations are also absent in the likely piscivorous tanysaurian *Austronaga minuta* (Wang et al., 2023a). At least three empty alveoli can be discerned, one between the two preserved teeth, and two posterior to the posteriormost preserved tooth. The tooth count of the premaxilla was therefore likely around 5–7. Tooth implantation is either subthecodont or thecodont (*sensu* Bertin et al., 2018) and the base of the crowns is not fused to the bone.

The lateral surface of the premaxilla is marked by a distinct fossa adjacent to the anteroventral margin of the external naris. The posterior end of the main body of the premaxilla is incomplete but likely did not extend much beyond its current preservation. The anterior margin of the premaxilla is rounded in lateral view, similar to the condition in *Pectodens zhenyuensis* (Li et al., 2017a). The prenarial process of the premaxilla is present and moderately well developed, but shorter than in *Dinocephalosaurus orientalis*, *Pectodens zhenyuensis*, and *Austronaga minuta* (Li, 2003; Li et al., 2017a; Wang et al., 2023a). By contrast, the prenarial process is absent in *Tanystropheus* spp. and *Macrocnemus* spp. (Spiekman et al., 2021b; Table 1). The prenarial process of *Trachelosaurus fischeri* is directed posterodorsally and forms a plate-like structure that only slightly reduces in transverse width posterodorsally, closely resembling the condition in *Dinocephalosaurus orientalis* and *Pectodens zhenyuensis* (Li, 2003; Li et al., 2017a). It has a rounded distal end. The postnarial process is broken off and mostly missing. The broadly rounded concavity between the prenarial process and main body of the premaxilla represents the margin of the external naris. It is large, and far displaced from the anterior margin of the premaxilla, similar to the condition in several tanystropheids and trachelosaurids (Spiekman et al., 2021b).

?Nasal. A plate-like element with a distinct tapering process preserved in MLU.GeoS.1612.D (Figs. 4; 5C) was previously tentatively identified as a parietal by Fischer but later reinterpreted as a jugal by Broili (Broili & Fischer, 1918). However, the morphology of this elongate, plate-like element does not correspond to the known morphology of either of these bones in early archosauromorphs. The identification of this element is hampered, because it is found in isolation and is incompletely

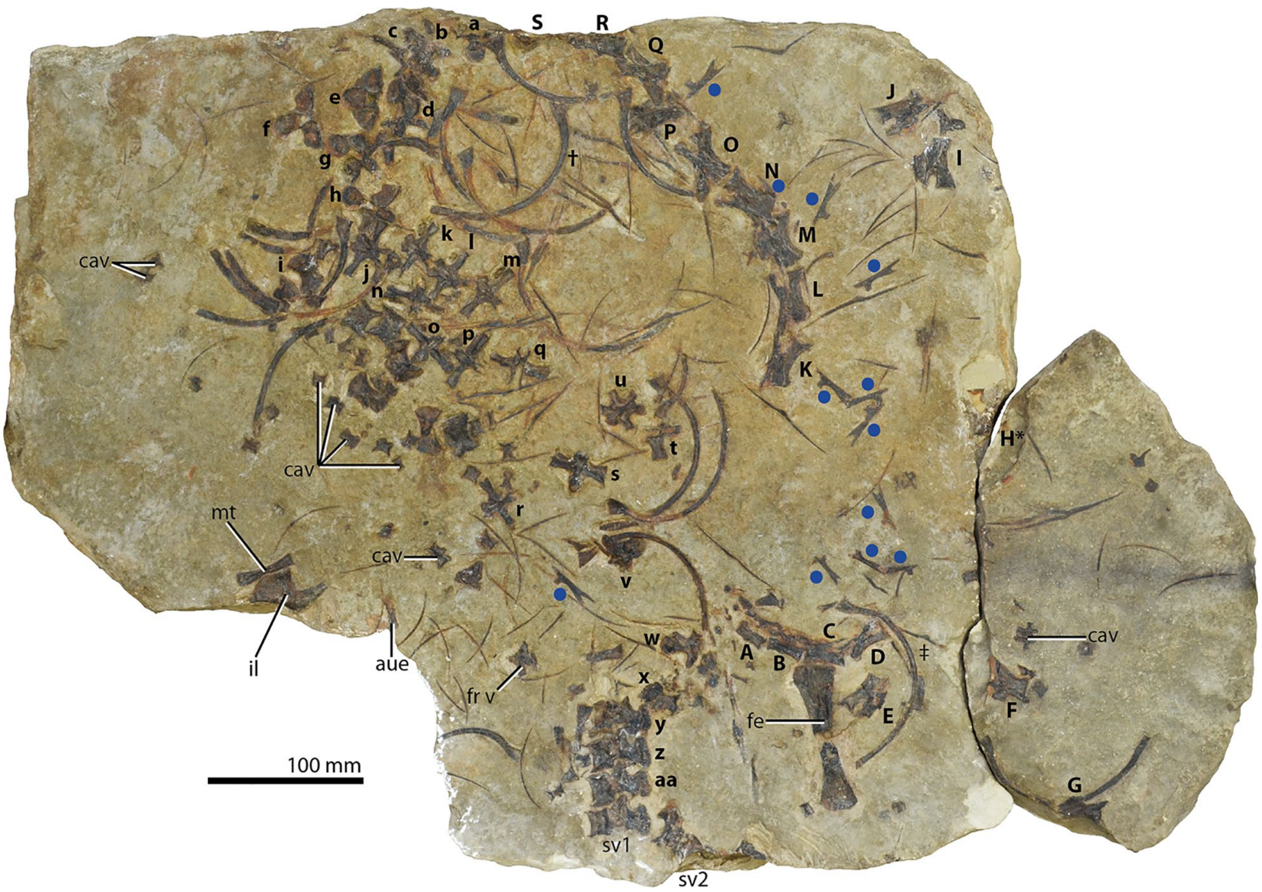

Fig. 3 Overview of MLU.GeoS.1612. A–B preserving the majority of the presacral vertebrae and appendicular elements. Cervical vertebrae are indicated with capitalised letters, dorsal and sacral vertebrae are indicated with lower case letters, blue dots indicate bifurcated cervical ribs. The element indicated with an asterisk represents a badly broken cervical vertebra, which could be identified based on plate 31 of Broili and Fischer (1918). The two ribs indicated with † and ‡, respectively, correspond to those listed in Table 4. Abbreviations: aue, autopodial element; cav, caudal vertebra; fe, femur; fr v, fragmentary vertebra; il, ilium; mt, metatarsal; sv, sacral vertebra

preserved, with most of its margins being broken. Furthermore, the overall morphology of *Trachelosaurus fischeri* appears to be quite derived, and therefore, its cranial morphology might have deviated considerably from that of other early archosauromorphs. It cannot be excluded that the bone represents a palatal element, but it is here considered to most likely represent a nasal. The nasal is large and plate-like in many early archosauromorphs (Ezcurra, 2016; Spiekman et al., 2021b), and the widely curved margin on one end of the element matches very well with the outline of an external naris. Therefore, this region of the element is interpreted as the anterior end of the nasal. Following this interpretation, the elongate and tapering anterior process of the bone could either represent the anteromedial process, which would have articulated with the prenarial process of the premaxilla, similar to the condition in *Macrocnemus* spp. (Jaquier et al., 2017), or it could represent the anterolateral process, which would have articulated with the maxilla ventrally, as in *Tanystropheus* spp. (Spiekman et al., 2020a).

?Postorbital. Near the putative nasal, another isolated skull bone is preserved (Figs. 4, 5D). It is triradiate, with a single concave margin that ends into two opposing, small processes, and a single, much larger process that is directed perpendicular to the concave margin. This larger process gradually tapers distally, giving it a triangular outline. This element might represent a postorbital. Following this interpretation, the concave margin is part of the orbital rim, and the larger process could represent the posterior process that would have articulated with the squamosal. The exposed surface is mostly smooth but shallowly depressed at the base of the larger process. If this element indeed is a postorbital, this would suggest that it is exposed in internal/medial view and thus represents the left postorbital.

?Postfrontal. An elongate, triradiate element is preserved in isolation adjacent to a gastralium in MLU.

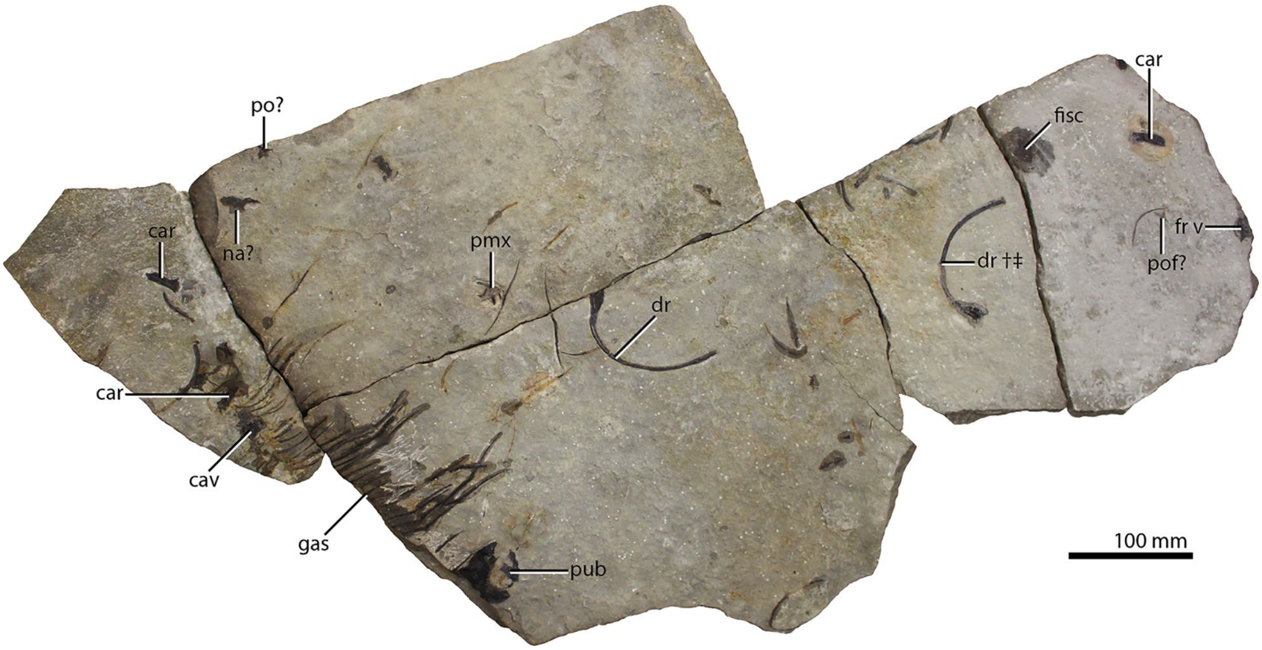

Fig. 4 Overview of MLU.GeoS.1612.C-G, preserving the cranial and proximal caudal remains, as well as a tentatively identified pubis and partial gastral basket. The rib marked with †‡ corresponds to the rib that is indicated the same in Table 4. Abbreviations: car, caudal rib; cav, caudal vertebra; dr, dorsal rib; fisc, fish scales; fr v, fragmentary vertebra; gas, gastralia; na, nasal; pmx, premaxilla; po, postorbital; pof, postfrontal; pub, pubis

GeoS.1612.G (Figs. 4, 5E). The largest process is both the longest and the widest. It maintains its transverse width for most of its length, but tapers from its distal third to a point. The other two processes are positioned on the other side of the element, one facing in an opposing direction to the largest process and the other process being almost perpendicular to the other two. Both smaller processes possess a sharp tip distally. The exposed surface of the element is mostly flat, except for a depression at the base of the two smaller processes. The shape of the element is somewhat reminiscent of a postfrontal, which is generally triradiate in early archosauromorphs. It specifically resembles the postfrontal of *Dinocephalosaurus orientalis* in possessing an elongate lateral process, and small anteromedial and posteromedial processes (Spiekman et al., 2024). Following this interpretation, the medial margin between the two smaller processes would have articulated with the frontal and parietal, whereas the elongate lateral process would have articulated with the postorbital.

Axial skeleton

Cervical vertebrae. In total, 19 associated postatlantal cervical vertebrae are confidently identified in MLU.GeoS.1612.A-B (Fig. 3) based on their morphology, comprising an elongate centrum with a markedly concave ventral margin in lateral view, and the presence of very closely associated para- and diapophyses on the ventrolateral side of the centrum near its anterior end, corresponding to the general cervical configuration in early archosauromorphs (Ezcurra, 2016; Spiekman et al., 2021b). One further, disarticulated cervical vertebra is now only preserved as a tiny, poorly preserved fragment (Fig. 3, indicated with H*). As is indicated in the plate of MLU.GeoS.1612.A-B in Broili and Fischer (1918, pl. 31), this element clearly represents a cervical vertebra that was well preserved prior to being heavily damaged at a later stage.

All cervical vertebrae are preserved in lateral view. The elements distributed over MLU.GeoS.1612.A-B comprise two articulated series and six isolated elements. The first articulated series is composed of four elements, preserved adjacent to the femur. The second series comprises nine elements and is interrupted posteriorly by the edge of the MLU.GeoS.1612.A slab, but if the curvature of the column is followed, it is clear that this section is still closely associated with the dorsal vertebrae preserved further posteriorly. Therefore, the posterior end of this series is positioned close to the end of the cervical column. Except for the anteriormost element, which is considerably smaller, the centra in the first series are 24–27 mm long, whereas most of those of the second series are approximately 33–35 mm long (Table 2). The centra of the isolated cervical vertebrae that could be measured are 27–31.5 mm long and are thus intermediate in size

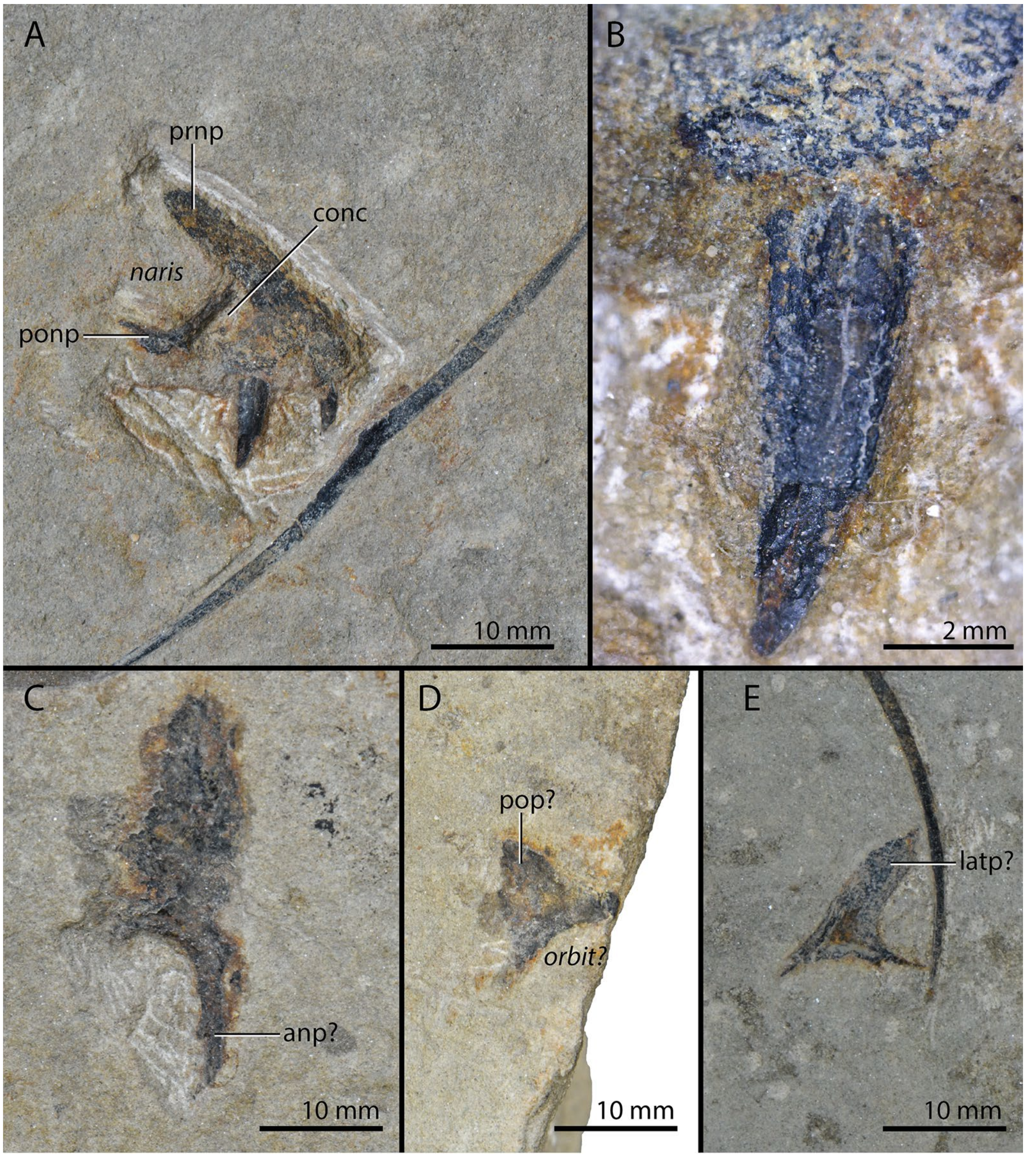

Fig. 5 Close-ups of the cranial elements of *Trachelosaurus fischeri*. **A** Right premaxilla in lateral view. **B** The posterior of the two preserved premaxillary teeth. **C** Possible nasal. **D** Possible postorbital. **E** Possible postfrontal. Abbreviations: anp, anterior process; conc, concavity; latp, lateral process; ponp, postnarial process; pop, posterior process; prnp, prenarial process

Table 1 Measurements of the cranial elements of MLU.GeoS.1612 in mm

	Main body anteroposterior length	Main body dorsoventral height	Prenarial process length	Prenarial process height at base	Largest tooth exposed height
Premaxilla	16.1*	4.3	8.6	3.8	6.7
	Maximum length				
?Nasal	32.1				
?Postorbital	12.1				
?Postfrontal	16.4				

Measurements of incomplete elements are marked with an asterisk (*)

between the vertebrae in the two articulated series. This gradual size increase from anterior to mid- to posterior cervical vertebrae is also observed in other tanysaurians, most notably *Dinocephalosaurus orientalis* (Spiekman et al., 2024). This suggests that all elements belong to the same individual, and therefore, that the neck of *Trachelosaurus fischeri* was composed of at least 20 cervical vertebrae (*cf.* Broili & Fischer, 1918; *contra* Huene, 1944).

The anteriormost, unambiguous cervical vertebra (Fig. 6A) is tentatively identified as the axis (*sec.* Broili & Fischer, 1918). It is considerably shorter than the succeeding vertebrae (Table 2), and the diapophysis is placed considerably further dorsally along the lateral surface of the centrum than in the postaxial anterior to mid-cervical vertebrae, matching the configuration of the axis in other early archosauromorphs, such as *Macrocnemus bassanii*, *Prolacerta broomi*, and *Azendohsaurus madagaskarensis* (Gow, 1975; Miedema et al., 2020; Nesbitt et al., 2015). The neural arch is fully detached from the centrum and a distinct longitudinal ridge along the dorsal margin of the centrum demarcates the position of the neurocentral suture. The ventral margin of the centrum is only weakly concave in lateral view compared to the postaxial cervical vertebrae. The neural arch is poorly preserved, but the postzygapophysis is distinct and strongly developed. An elongate, plate-like element positioned anterodorsal to the axial neural arch could represent one of the atlantal neural arches, but it is too poorly preserved to ascertain this confidently. Several small, scattered remains are preserved anterior to the axis. Broili and Fischer (1918) considered these to be remains of the atlas. They are too poorly preserved to corroborate this confidently, and at least one element appears to be a fish scale, but some elements could indeed belong to the atlas based on their overall size and position.

In addition to their anteroposterior length, the height of the neural spine also seems to gradually increase posteriorly in the cervical vertebrae (Table 2), although the spinous process is covered by sediment in most of them and these, therefore, could not be measured. The anterior articular surface of the centrum is positioned slightly dorsally to the posterior articular surface (Fig. 6C), as is the case in many early archosauromorphs (Ezcurra, 2016). From the concave outline of both articular surfaces of the centrum as exposed in certain elements, it can be discerned that the cervical vertebrae were amphicoelous. The parapophysis is positioned on the anteroventral edge of the centrum in lateral view. The diapophysis is positioned dorsally and slightly posteriorly to the parapophysis and it is placed on a short, wing-like process that gradually fades posterodorsally along the lateral surface of the centrum. The neural arches lack laminae. The zygapophyses are well developed and epipophyses are present dorsal to the postzygapophyses, as occurs in most non-eucrocopodan archosauromorphs (Ezcurra, 2016; Ezcurra et al., 2023). The posterodorsal extent of the epipophyses is not preserved in any of the elements. There is no fossa lateral to the base of the neural spine. The neural spine is dorsoventrally short, similar to the general condition in tanystropheids and trachelosaurids, except for *Tanystropheus* spp. and *Sclerostropheus fossai*, in which the neural spine is almost completely reduced (Spiekman & Scheyer, 2019; Spiekman et al., 2021b). The anterior and posterior margins of the neural spines are both concave in lateral view, as is the common condition in early archosauromorphs, although in the trachelosaurids *Dinocephalosaurus orientalis*, *Austronaga minuta*, and *Pectodens zhenyuensis*, the neural spine is trapezoidal in outline in lateral view (Li et al., 2017a; Spiekman et al., 2024; Wang et al., 2023a). The distal ends of the exposed neural spines are gently convex in lateral view, and they are transversely expanded, forming a strongly rugose thickening. A distal transverse thickening of the neural spine also occurs in *Augustaburiania vatagini*, *Czatkowiella harae*, *Gracilicollum latens*, *Macrocnemus* spp., and *Tanystropheus "conspicuus"* among non-crocopodan archosauromorphs (Borsuk-Białynicka & Evans, 2009; Scheyer et al., 2020; Sennikov, 2011; Wang et al., 2023b; Wild, 1973), but the degree of rugosity present in

Table 2 Measurements of the cervical vertebrae (CV) preserved on MLU.GeoS.1612.A-B in mm

Cervical vertebra	Centrum total length	Height posterior articular surface of centrum	Height neural spine
CV A	19	–	–
CV B	24.5	10.2	–
CV C	26.8	–	–
CV D	26.4	7.9?	–
CV E	26.9	11.2	7.6
CV F	–	–	8
CV G	–	–	7.9
CV H	–	–	–
CV I	31	13.9	10.1
CV J	31.5	13.8	–
CV K	34.5	15	–
CV L	34.2	11.6	–
CV M	34.1	11.9	10.9
CV N	34.2	14.3	–
CV O	32.9	11.9	–
CV P	–	–	–
CV Q	30.9	–	–
CV R	–	–	–
CV S	–	–	–

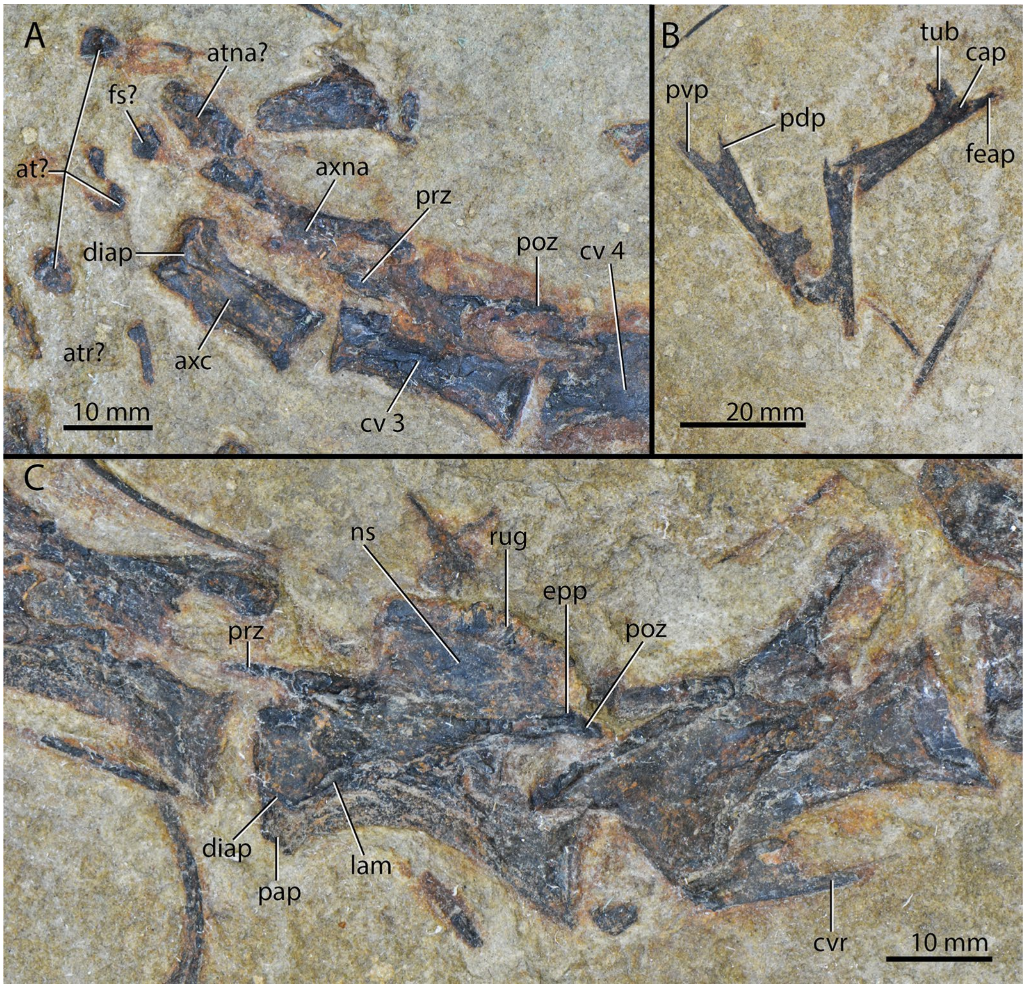

Fig. 6 Close-ups of selected cervical vertebrae and ribs of *Trachelosaurus fischeri*. **A** Anteriormost preserved cervical vertebrae (elements A–C), including the tentatively identified axis and possible atlantal elements. **B** Cervical ribs with bifurcating distal ends. **C** Mid-cervical vertebrae (elements L–N). Abbreviations: at, atlantal element; atna, atlantal neural arch; atr, atlantal rib, axc, axis centrum; axna, axis neural arch; cap, capitulum; cv, cervical vertebra; cvr, cervical rib; diap, diapophysis; epp, epipophysis; feap, free-ending anterior process; fs, fish scale; lam, lamina; ns, neural spine; pap, parapophysis; pdp, posterodorsal process; poz, postzygapophysis; prz, prezygapophysis; pvp, posteroventral process; rug, rugosity; tub, tuberculum

Trachelosaurus fischeri is considerably more extensive. There are no intercentra between the vertebrae.

Cervical ribs. Twelve cervical ribs are present on MLU.GeoS.1612.A, including a single partial rib preserved in articulation with its corresponding vertebra; its shaft is oriented parallel to the vertebral column (Fig. 6C). At least one additional rib was previously present within the now missing rock fragment located at the intersection between MLU.GeoS.1612.A and B (see Broili & Fischer, 1918, pl. 31, between the cervical vertebrae "9" and "10" therein). All cervical ribs possess a short shaft, not or barely exceeding the length of its corresponding vertebra, which bifurcates distally into two distinct prongs (Fig. 6B). This represents a configuration unique among Permo-Triassic archosauromorphs. The ribs possess a distinct anterior free-ending process as in other archosauromorphs, which terminates in a blunt tip. Although prominent, this anterior process is not as long as those seen in *Czatkowiella harae*, *Sclerostropheus fossai*, *Tanytrachelos ahynis*, *Ozimek volans*, *Pectodens zhenyuensis*, *Dinocephalosaurus orientalis*, *Austronaga minuta*, and *Gracilicollum latens* (Spiekman et al., 2021b; Wang et al., 2023a, 2023b). The tubercular and capitular heads of the cervical ribs are positioned closely to each other, as in other early archosauromorphs. The tuberculum forms a prominent process that is rectangular in outline in lateral view, whereas the capitulum only forms a small knob-like protrusion. The rib shaft is lateromedially thin, forming only a lamina between the slightly thickened dorsal and ventral margins. However, the shaft is of considerable height dorsoventrally, giving it a stocky appearance in lateral view. The dorsal margin of the shaft is concave proximally and straight distally, where it is oriented posteriorly and slightly dorsally. The ventral margin of the shaft is straight and would have been oriented parallel to the vertebral column. Consequently, the rib shaft is slightly constricted directly posterior to the tuberculum in lateral view, before widening dorsoventrally further posteriorly. The distal bifurcation of the shaft is formed by posterodorsal and posteroventral prongs, of which the latter extends further posteriorly. Both ends terminate in a sharp tip. They are separated from each other by a well-rounded and deep posterior notch in lateral view.

Dorsal vertebrae. The post-cervical vertebrae are distributed mainly over MLU.GeoS.1612.A. They are disarticulated, except for an articulated series of four elements that are exposed in left lateral view near the edge of the slab (Fig. 3). Due to the disarticulation of the vertebral column, the exact order of the vertebrae cannot be reconstructed. However, the vertebrae are still generally associated in an anterior-to-posterior sequence, which is also corroborated by a gradual morphological shift in the width of the transverse processes, which are very wide laterally in the anterior dorsal vertebrae and which gradually narrow posteriorly (Table 3). Furthermore, the anterior part of the dorsal column is still closely associated with the posterior end of the cervical series, even though the exact cervical–dorsal transition is not preserved. The disarticulated vertebrae are exposed under various angles. The articulated series of four elements and a single displaced element positioned directly posterodorsally to this series represent the posteriormost preserved elements in MLU.GeoS.1612.A (Fig. 7D). The preceding elements can be unambiguously identified as dorsal vertebrae due to the morphology of their transverse processes (Fig. 7A, B). However, in these posteriormost elements, no clear transverse processes can be discerned (Fig. 7D). They have either broken or eroded away due to their angle of preservation, or, more likely, the transverse process was incipient and the rounded, slightly concave surface on their lateral sides represent large rib facets. Because of this morphology, it is difficult to determine whether they represent posterior dorsal, sacral, and/or anterior caudal vertebrae, as was also the consideration of Broili and Fischer (1918). Based on the comparatively large size of its inferred rib articulation site, the posteriormost preserved element in the series is identified as a sacral vertebra, and therefore, the preceding elements represent posterior dorsal vertebrae (*contra* Huene, 1944, who interpreted these elements as proximal caudal vertebrae, with only the anteriormost element being considered as a potential sacral vertebra). In agreement with our interpretation, the vertebrae anterior to the probable first sacral vertebra possess posterior centrodiapophyseal, prezygodiapophyseal and postzygodiapophyseal laminae, supporting their identification as dorsal elements. Consequently, 27 dorsal vertebrae are preserved in MLU.GeoS.1612.A based on this interpretation, whereas Broili and Fischer (1918) estimated the total number of dorsal and possibly sacral vertebrae at around 20 to 21. *Dinocephalosaurus orientalis* possesses 28 or 29 dorsal vertebrae (Spiekman et al., 2024), whereas the trunk of other early archosauromorphs is generally restricted to 12 to 18 dorsal vertebrae (Spiekman et al., 2021b); the trachelosaurid *Pectodens zhenyuensis* has only 13 to 14 dorsal vertebrae (Li et al., 2017a).

The anteriormost dorsal vertebrae that exhibit clear morphological details are exposed in either anterior or posterior view (Fig. 7A). The articular surfaces of their centra are slightly concave, suggesting that they are platycoelous to amphicoelous. The articular surfaces are dorsoventrally taller than transversely wide, and their ventral margins are strongly rounded. The neural canal is rectangular in outline; it is roughly square in the most anterior of the elements exposing this feature, whereas in the subsequent elements, it is considerably transversely narrower, resulting in a tall, columnar opening. Only fragments of the neural spine are preserved in these anterior elements, and they were likely relatively low. As mentioned above, the transverse processes in these elements are laterally very wide, being almost three times wider than the height of the articular surface of their corresponding centrum (Table 3). In the anteriormost element preserving fully exposed transverse processes (Fig. 3, indicated with e), the dorsal margin of the transverse process slopes gently lateroventrally in anterior or posterior view, whereas in the subsequent elements, the transverse process is fully laterally oriented and its dorsal margin is gently convex. Furthermore, a thin dorsoventrally oriented lamina projects from the transverse process of this element, providing the process a marked wing-like outline in anterior or posterior view. The lateral margin of this lamina is distinctly convex, and it curves ventromedially, terminating ventrally on the ventral portion of the lateral surface of the centrum. The subsequent vertebrae exhibit a similar lamina, but in these elements, the ventral margin of this lamina is distinctly concave, and the lamina terminates more dorsally than in the anteriormost element. Such a prominent lamina extending from the transverse process of the dorsal vertebrae is unusual among non-archosaurian archosauromorphs, but it does occur in *Dinocephalosaurus orientalis* (Spiekman et al., 2024).

Table 3 Measurements of the dorsal vertebrae (DV) and sacral vertebra (SV) preserved on MLU.GeoS.1612.A-B in mm

Vertebra	Width across transverse processes	Length across zygapophyses	Height at posterior or anterior edge centrum	Height neural spine	Centrum length
DV a	–	–	–	–	–
DV b	–	–	–	–	–
DV c	–	–	–	–	–
DV d	–	–	15.5	–	–
DV e	42.2	–	15.1	–	–
DV f	41.1	–	15.2	–	–
DV g	43.2	–	15.8	–	–
DV h	42.6	–	16.7	–	–
DV i	–	–	–	–	–
DV j	42.8	25.8	–	–	–
DV k	42.2	25.2	–	–	–
DV l	37.1	28.1	–	–	–
DV m	42.8	24.8	–	–	–
DV n	41.1	21.7	–	–	–
DV o	40.6	–	–	–	–
DV p	40.9	21.4	–	–	–
DV q	38.2	24	–	–	–
DV r	37	22.7	–	–	–
DV s	36.9	–	–	–	–
DV t	34.2	–	–	–	16.07
DV u	28.1	26.8	–	–	–
DV v	–	–	–	–	–
DV w	–	–	–	–	–
DV x	–	–	–	–	–
DV y	–	26.8	16.2	–	17.8
DV z	–	23.9*	16.7	13.8	18.4
DV aa	–	23.4*	16.8	12.6	20.0
SV 1	–	25.1*	15.4	13.8	15.3
SV 2	–	23.9*	13.3*	15.4	16.6

Measurements of incomplete elements are marked with an asterisk (*)

Further posteriorly, in the elements that are interpreted here as mid-dorsal vertebrae, the neural arch and centra have disarticulated from each other (Fig. 7A); their neurocentral suture was therefore clearly not fused. The neural arches are generally exposed in either dorsal or ventral view, whereas the centra are mostly roughly exposed in lateral view. The centra appear to be transversely constricted, particularly in their anteroposterior midpoint, giving the element an hourglass-shaped outline in dorsal view or ventral view. This feature is likely exaggerated by diagenetic compaction. The ventral margin of the centrum is strongly concave in lateral view, and the articular surfaces are again platycoelous to amphicoelous. The transverse processes in these elements are restricted to the neural arch. As in the anterior dorsal vertebrae, these processes are well developed laterally, which is an uncommon feature among non-archosaurian archosauromorphs. A similar transverse extent of these processes can only be found in *Pectodens zhenyuensis*, in which they are considerably more slender (Li et al., 2017a). The transverse processes are projected directly laterally. In dorsal or ventral view, the anterior and posterior margins of the process are gently concave and the distal end, which forms the articular surface for the rib, is anteroposteriorly expanded and laterally flat. Due to the angle of preservation, the ventral lamina of the transverse process is only poorly exposed in this section of the dorsal column. However, it is still clearly present in these elements, albeit more dorsally restricted than in the anterior dorsal vertebrae. The zygapophyses are generally poorly preserved. As in other archosauromorphs, the postzygapophyses are considerably larger than the prezygapophyses, being both transversely wider and anteroposteriorly longer. The neural spine is not preserved in most mid-dorsal vertebrae. However, in some elements, which are preserved under a slight angle from the dorsoventral

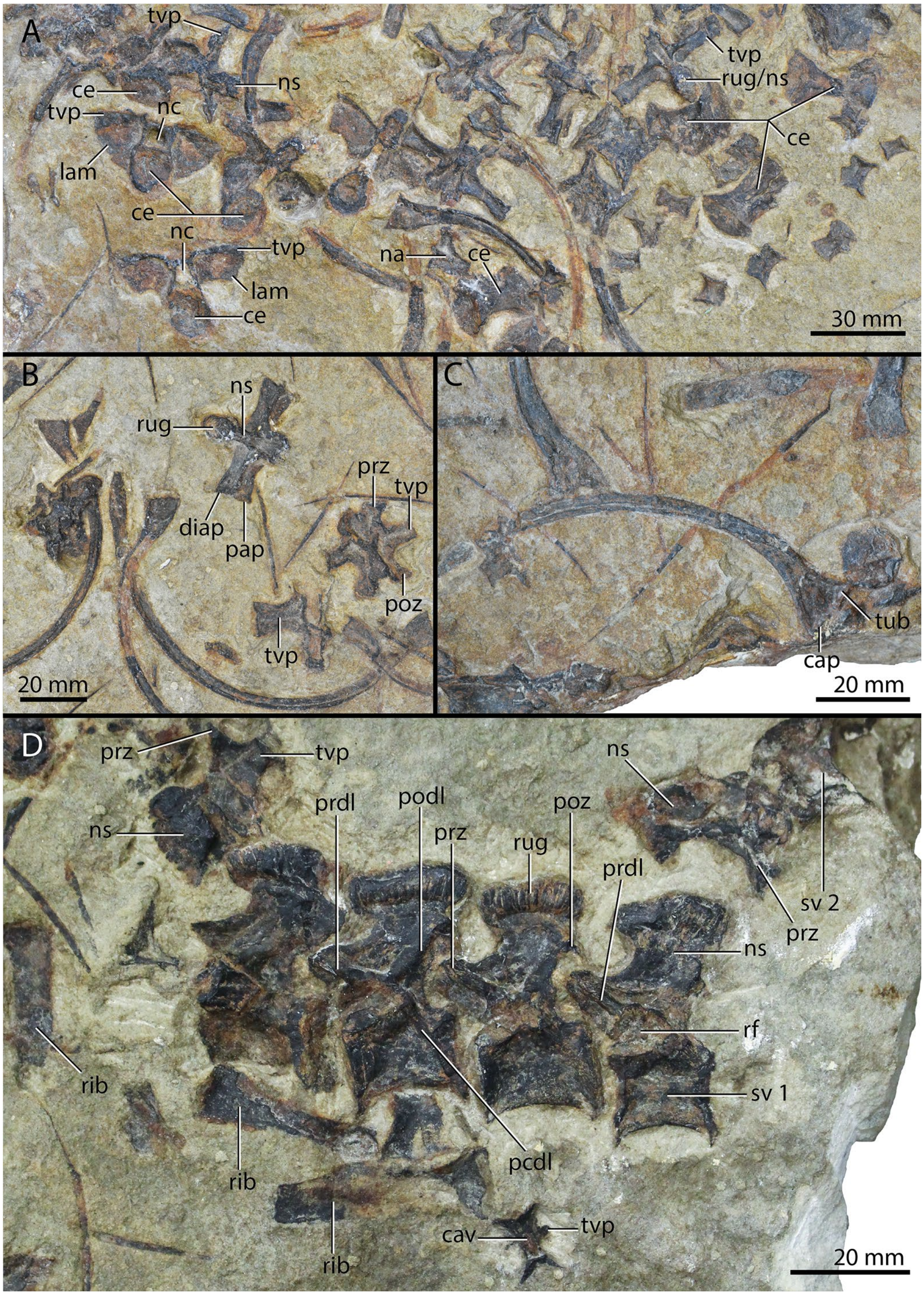

Fig. 7 Close-ups of selected dorsal and sacral vertebrae and ribs of *Trachelosaurus fischeri*. **A** Anterior and mid-dorsal vertebrae (elements a-o). **B** Posterior dorsal vertebrae (elements s-u). **C** Anteriormost dorsal rib. **D** Posteriormost dorsal vertebrae and sacral vertebrae. Abbreviations: cap, capitulum; ce, centrum; diap, diapophysis; lam, lamina; na, neural arch; nc, neural canal; ns, neural spine; pap, parapophysis; pcdl, posterior centrodiapophyseal lamina; podl, postzygodiapophyseal lamina; poz, postzygapophysis; prdl, prezygodiapophyseal lamina; prz, prezygapophysis; rf, rib facet; rug, rugosity; sv, sacral vertebra; tub, tuberculum; tvp, transverse process

plane, the neural spine is present but deformed. It is shorter than the height of the articular surface in the corresponding centra. It expands gradually transversely towards its distal end and has a more extensively rugose distal margin than the cervical vertebrae. Even though *Tanystropheus* spp., *Dinocephalosaurus orientalis*, and *Ozimek volans* also possess a transverse expansion on the distal end of the dorsal neural spines, the expansion is considerably more extensive in *Trachelosaurus fischeri* (Spiekman et al., 2021b). Furthermore, the rugosity present on the distal margin of the neural spines, including vertically oriented striations in some vertebrae, is more reminiscent of that present in certain marine diapsids like *Claudiosaurus germaini* and *Augustasaurus hagdorni* (Carroll, 1981; Sander et al., 1997) rather than early archosauromorphs. A much smaller amount of rugosity only occurs on the spine tables of the dorsal vertebrae of *Dinocephalosaurus orientalis* among non-archosauriform archosauromorphs (Spiekman et al., 2021b, in press). The distal surface of the neural spine in *Trachelosaurus fischeri* is gently convex.

The transverse processes start to distinctly, but gradually, reduce in transverse width from about vertebra q onwards (Fig. 3). Postcervical vertebra x (Fig. 3) is the last element to unambiguously possess a transverse process. It is preserved in close association with the subsequent vertebra, which is the anteriormost element in the fully articulated series of four vertebrae exposed in left lateral view (Fig. 7D). The ventral margins of the centra in this series are weakly concave in lateral view, to a lesser extent than the mid-dorsal centra. The centra are slightly longer than tall and lack a lateral fossa. The posterior articular surface of the centrum of the anteriormost element of this series is partially exposed. It is similar to the preceding dorsal vertebrae, being taller than wide with a slightly concave surface. No suture line for the neurocentral suture can be discerned in this series of vertebrae. In the second element of the series and to a lesser extent in the third, the distal end of a poorly developed posterior centrodiapophyseal lamina and clear prezygodiapophyseal and postzygodiapophyseal laminae are present; a prezygodiapophyseal lamina can also be discerned on the final vertebra of the series, the probable first sacral element. An elongate, strut-like element is preserved directly ventral to the anteriormost element of the series. This was interpreted as a haemal arch by Broili and Fischer (1918). However, based on its morphology and relatively wide and flat proximal end, it is most likely a short "lumbar" rib, and thus, the corresponding element is a posterior dorsal vertebra. Another, disarticulated, "lumbar" rib is present somewhat anterior to the same vertebra. The postzygapophyses of these vertebrae are positioned on a considerably higher dorsoventral level than the prezygapophyses. The postzygapophyses are oriented posteriorly and slightly dorsally, whereas the prezygapophyses are of considerable length and oriented anterodorsally. There is no fossa lateral to the base of the neural spine. The distal region of the neural spines expands anteriorly and posteriorly in lateral view. The rugosity of the transversely expanded distal end of the neural spines is composed of clear striations, marked by dorsoventrally oriented grooves in lateral view.

Dorsal ribs. More than 20, mostly disarticulated, dorsal ribs are preserved in MLU.GeoS.1612.A-B (Fig. 3). Three further dorsal ribs are present in the MLU.GeoS.1612.C, E–F (Fig. 4), of which two are largely complete and a third preserves the distal end of a shaft. The anteriormost preserved dorsal rib in MLU.GeoS.1612.A is found in articulation with a small fragment of an anterior dorsal vertebra (Fig. 7C). The tuberculum and capitulum of this rib are separated from each other by a very small concave gap between them. All subsequent ribs, including the element far displaced and preserved in MLU.GeoS.1612.F, are holocephalous and the single head of the ribs becomes gradually narrower in more posterior elements. The anteriormost dorsal ribs are slightly shorter than those in the mid section of the trunk (Table 4). The dorsal rib shafts have a strong curvature in anterior or posterior view, and therefore, the torso of *Trachelosaurus fischeri* was barrel-shaped, as was also observed by Broili and Fischer (1918). The shaft maintains its width along its entire width and terminates distally in a blunt tip. A distinct groove is present along the surface of the shaft in most ribs.

Sacral vertebrae. The probable first sacral vertebra is preserved in articulation with the last three dorsal vertebrae. The morphology of the element resembles that of the posteriormost dorsal vertebrae (see above) with the exception of the presence of a larger rib facet that is situated on both neural arch and centrum, as occurs in the sacral vertebra of other early archosauromorphs (Fig. 7D). Posterodorsal to the inferred first sacral vertebra, another element is preserved. Like the preceding vertebrae, it is exposed in left lateral view, but it is poorly preserved and much of its left lateral surface is broken. This likely represents the second sacral vertebra, but it does not provide further useful information. No sacral ribs are preserved.

Caudal vertebrae and ribs. Elements of the caudal vertebrae are preserved across MLU.GeoS.1612.A-C, G. The most anterior elements are preserved in association in MLU.GeoS.1612.C adjacent to the partially articulated gastral basket. They comprise at least two very poorly preserved centra, a single, more complete vertebra, and three relatively well-preserved caudal ribs (Fig. 8). The most complete vertebra (β) is exposed in lateral view and

Table 4 Measurements of selected dorsal ribs in MLU.GeoS.1612 in mm

	Total length
Dorsal rib †	137.5
Dorsal rib ‡	146.5
Dorsal rib †‡	147.2

The symbols of the ribs correspond to those used to highlight these respective ribs in Figs. 4 and 5

has a very gently concave ventral margin. It is quite short anteroposteriorly (Table 5). The neural arch is poorly preserved and likely mostly comprises a transverse process that has been shifted relative to the centrum, so that it is exposed in ventral view. The outline of the transverse process is subrectangular, being longer lateromedially than wide anteroposteriorly. One of the caudal ribs, which is preserved distal to the transverse process, likely disarticulated from this vertebra. Based on the width of the transverse process and the vicinity of the caudal rib, the vertebra is identified as a proximal caudal element. The preserved caudal ribs on MLU.GeoS.1612.C vary in length but all are relatively stocky elements that maintain their width along most of their length.

The remains of at least 20 caudal vertebrae are exposed in the MLU.GeoS.1612.A-B (Fig. 3). Most of these elements are represented by isolated centra that are scattered across MLU.GeoS.1612.A, adjacent to the dorsal vertebrae and the ilium. They slightly decrease in size in the opposite direction of the dorsal vertebrae on the slab. Only the anteriormost element on MLU.GeoS.1612.A preserves remnants of transverse processes, which are very poorly developed (Fig. 7D). The remaining elements do not appear to have possessed transverse processes, and they are therefore interpreted as distal caudal vertebrae, an identification that agrees with their diminutive size. A single, poorly preserved neural arch, exposed in dorsal view, is present on MLU.GeoS.1612.B. Its neural spine is mostly broken. Parts of an additional vertebra are located on both sides of the crack delimiting MLU.GeoS.1612.A and B. Transverse processes, relatively much longer in the latter element, are present in both of these vertebrae, suggesting that they represent middle caudal vertebrae.

Gastralia. A large articulated, partial gastral basket is preserved across MLU.GeoS.1612.C-E (Figs. 4, 8). The gastralia are closely packed together. In addition, a large amount of disarticulated gastralia are scattered across all slabs (Fig. 2B), indicating the presence of a very extensive gastral basket in agreement with the large dorsal vertebral count. They are all elongate, slender elements, similar to those seen in early archosauromorphs generally (Ezcurra, 2016). Two distinct types are present. The first type constitutes relatively smaller elements that have a gently continuous curvature. The second, larger type, represents elements that are slightly bowed, resulting in a gentle V-shaped outline. A few of the latter type possess two long prongs on one side. These elements thus have the outline of a two-pronged fork. In the partial gastral basket, the smaller, lateral elements articulate on either side of a larger, V-shaped element. The lateral gastral elements medially approach, but do not reach, the bend of the larger elements.

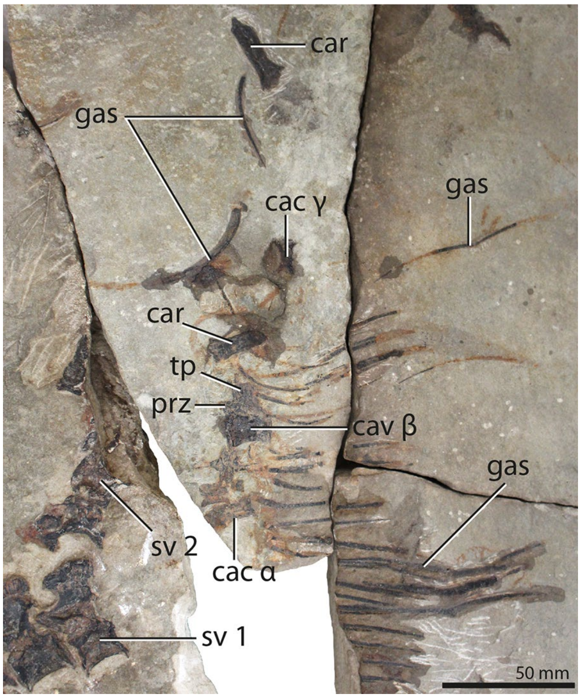

Fig. 8 Close-up of the proximal caudal region and partial gastral basket of *Trachelosaurus fischeri*. The caudal centra marked with α, β, and γ correspond to the elements that are indicated the same in Table 5. Abbreviations: cac, caudal centrum; car, caudal rib; cav, caudal vertebra; gas, gastralia; prz, prezygapophysis; sv, sacral vertebra; tp, transverse process

Table 5 Measurements of the caudal vertebrae preserved on MLU.GeoS.1612.C in mm

	Total centrum length
Caudal α	15.7
Caudal β	17.2
Caudal γ	12.8

The symbols of the caudal vertebrae correspond to those used to highlight these respective vertebrae in Fig. 8

Appendicular skeleton

Ilium. A right ilium is preserved near the edge of MLU.GeoS.1612.A. It is exposed in lateral view and virtually complete, only missing the posteriormost end of the postacetabular process (Fig. 9A). The supra-acetabular crest is either poorly developed or strongly diagenetically compressed and only a slight convexity is present at the dorsalmost level of the acetabulum, resembling the condition in non-eucrocopodan archosauromorphs (Ezcurra et al., 2023). The main body of the ilium is sloped on each side in lateral view, anteroventrally on the anterior margin and posteroventrally on the posterior margin, with the latter forming the steepest angle with the horizontal plane. There is no posterior heel on the distal end of the ischiadic peduncle. The ventral margin of the ilium is subtriangular, and the articular surfaces for the pubis and ischium are subequal in anteroposterior length. There is no ridge on the lateral surface of the iliac blade and, although it is damaged, the dorsal margin seems to have been continuously convex. The postacetabular process is mostly posteriorly, and also slightly dorsally, oriented and gradually reduces its dorsoventral height posteriorly. The ventral half of the lateral surface of the postacetabular process lacks the depression present in several tanystropheids (Ezcurra, 2016). A preacetabular process is absent, as is the case in *Dinocephalosaurus orientalis* (Spiekman et al., 2024), and consequently, the anterior margin of the iliac blade is gently rounded. A tuber on the anterior margin of the iliac blade, a feature previously identified in *Tanystropheus longobardicus*, *Raibliania calligarisi*, *Fuyuansaurus acutirostris*, the Hayden Quarry tanystropheid, and some specimens of *Macrocnemus bassanii* (*sensu* Pritchard et al., 2015; see also character 266 of Spiekman et al., 2021b for further explanation of this feature), is absent in *Trachelosaurus fischeri*.

Pubis. A large, incomplete, and poorly preserved element was tentatively identified as a pubis by Huene (1902) and a coracoid by Broili and Fischer (1918). It is here identified as a right(?) pubis. The element has a rounded outline, with a single, relatively flat, margin, and a distinct pubic foramen (Fig. 9C). This configuration corresponds closely with the rounded pubis present in *Dinocephalosaurus orientalis* (Spiekman et al., 2024). The pubis is found adjacent to the associated gastral basket at the edge of MLU.GeoS.1612.E in relatively close proximity to the sacral series, ilium, and hind limb elements (Fig. 2B).

Femur. A large, robust element is preserved adjacent to the anterior cervical vertebrae in MLU.GeoS.1612.A (Fig. 9B). It is strongly crushed due to diagenetic compression and its surface is highly fractured. The element is broken in two pieces, with the central portion of the shaft missing, but it is preserved as a natural mould. This element is identified as a left femur (*sec.* Huene, 1902, 1944; Broili & Fischer, 1918). It lacks distinct condyles on both the proximal and distal ends, as well as the sigmoid or curved shape present in the femora of most terrestrial neodiapsids. Instead, the shaft is straight. The shape and proportions of this element are similar to the femur of *Dinocephalosaurus orientalis*, in which the reduction of the above-mentioned features is related to the formation of flipper-like limbs for aquatic propulsion (Chen et al., 2014; Spiekman et al., 2024). The widths of both ends of the element roughly correspond with the width of the acetabulum as preserved on the ilium (Table 6), providing additional evidence that it represents a femur. One edge of the element is distinctly raised relative to the rest of the bone, and this is tentatively identified as an internal trochanter. Based on this interpretation, the bone represents the left femur with the widest end, positioned adjacent to the anterior cervical vertebrae, identified as the proximal end. From the proximal end, the element gradually reduces in width until about two-thirds along the length of the shaft. From there, the shaft increases in width again to the expanded distal end. The proximal end is slightly wider than the distal end. The exposed proximal margin is roughly straight, whereas the distal margin is gently and continuously convex. No distinct medullary cavity appears to be present on either of the exposed sides of the broken shaft, although this could be the result of the strong compression of the bone.

Metatarsal. An elongate, pillar-like element is preserved directly adjacent to the ilium in MLU.GeoS.1612.A (Fig. 9A). Based on its relative size and elongation, as well as its location adjacent to the ilium, it most likely represents a metatarsal (*sec.* Huene, 1944). Broili and Fischer (1918) identified this element as either a metatarsal or metacarpal. The ends are roughly straight to slightly convex and they are slightly expanded relative to the shaft, with one end, presumably the proximal end, being slightly more expanded.

A similar but considerably smaller and incomplete element is preserved near the edge of the slab, posterior to the ilium (Fig. 3). Based on its considerably smaller size, yet similar pillar-like morphology, this element could represent a metatarsal (e.g., metatarsal I), a metacarpal, or a phalanx.

Unidentified remains

Several other remains preserved on MLU.GeoS.1612 can be assigned to *Trachelosaurus fischeri* based on their relative size and type of preservation. However, these elements could not be identified because of the lack of preserved diagnostic features (Figs. 3, 4).

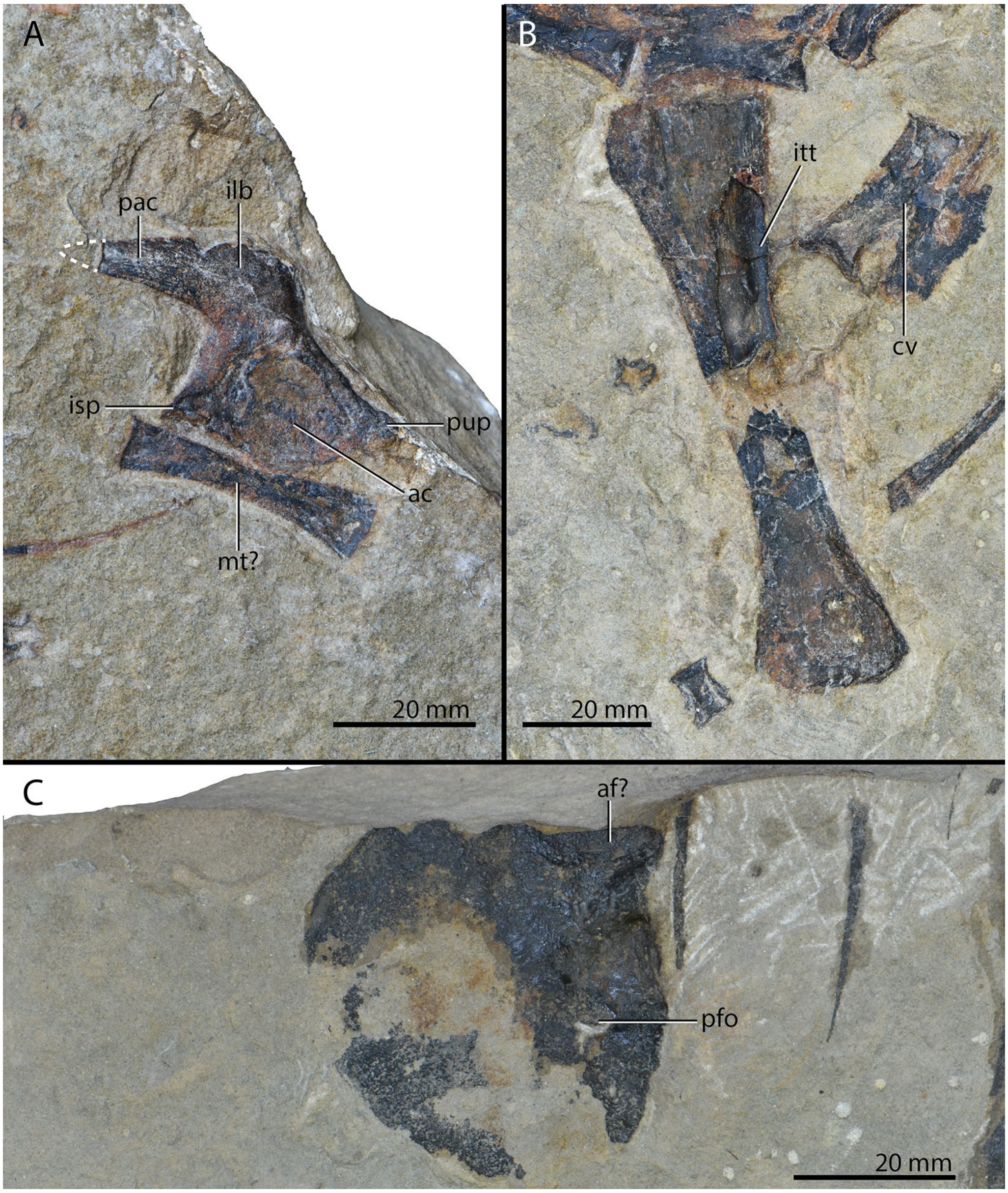

Fig. 9 Close-ups of the appendicular elements of *Trachelosaurus fischeri*. **A** Right ilium in lateral view and tentatively identified metetarsal. **B** Left femur in ventral view. **C** Right (?) pubis in medial(?) view. Abbreviations: ac, acetabulum; af, articular facet; cv, cervical vertebra; for, foramen; ilb, iliac blade; isp, ischial peduncle; itt, internal trochanter; mt, metatarsal; pac, postacetabular process; pfo, pubic foramen; pup, pubic peduncle

Phylogenetic results

Spiekman et al. (2021b) **matrix.** The SCT is generated from 52 MPTs of 1240 steps recovered in the equal weights analysis. It is poorly resolved, with a massive polytomy composed of all members of Tanysauria, in which only the internal relationships within Trachelosauridae are resolved (Additional file 1). The application of the iterPCR protocol resulted in the pruning a posteriori of *Sclerostropheus fossai*, *Raibliania calligarisi*, *Augustaburiania vatagini*, *Elessaurus gondwanoccidens*, *Fuyuansaurus acutirostris*, and *Gracilicollum latens*. The resulting RSCT recovered a large tanystropheid clade (Fig. 10A). Together with Trachelosauridae, Tanystropheidae forms the more inclusive Tanysauria, a clade that was also recovered as monophyletic in previous iterations of this matrix (Spiekman et al., 2021b, 2024; Lu & Liu, 2023; Wang et al., 2023a, 2023b). Tanysauria has the following synapomorphies in all the MPTs: premaxilla without a palatal shelf on its medial surface (character 11: 1 → 0), a thick anterior margin of the premaxilla results

Table 6 Measurements of the appendicular elements in mm

	Main body maximum length	**Maximum height**	**Acetabulum maximum length**	**Dorsal blade anteroposterior length**
Ilium	35.8	32.3	23.1	32.3*
	Maximum length	**Maximum height**		
Pubis	42	43		
	Total length	**Width at ?proximal end**	**Width at ?distal end**	**Width at around midshaft**
Femur	99	24.9	24.1	11.4
	Total Length	**Maximum width (proximal end?)**		
Metatarsal	38.1	10.3		
Autopodial element	21	7		

Measurements of incomplete elements are marked with an asterisk (*)

in the external nares being posteriorly displaced (character 31: 0 → 1), postaxial intercentra absent (character 182: 0- > 1), axis neural spine expanded anterodorsally in lateral view (character 186: 0 → 1), parapophysis of posterior dorsal vertebrae positioned entirely on neural arch (character 212: 0 → 1), ratio of anteroposterior length of vertebral centrum versus proximodistal length of corresponding haemal spine in anterior caudal elements between 0.64–0.81 (character 224: 0 → 1), scapular blade largely posteriorly directed and semi-circular in outline with a continuously curved anterior/dorsal margin (character 228: 0 → 1), humerus without thick subcilindrical tuberosity on ventral margin of the deltopectoral crest (character 244: 0 → 1), ratio of width of the distal end of the metacarpal I versus its total length between 0.38 and 0.43 (character 259: 0 → 1), and only one element of distal tarsals 1 and 2 present in mature individuals (character 292: 0 → 1). Tanystropheidae possesses the following synapomorphies common to all MPTs: haemal spine maintains breadth along its length (character 223: 2 → 1), ilium with low brevis shelf (character 269: 0 → 1), and ratio of length of metatarsal IV versus proximodistal length of metatarsal V between 3.65 and 5.15 (character 305: 1 → 3).

Although the topology of the tanystropheid clade is generally similar to the recent results in Spiekman et al. (2024), there are some notable differences. Compared to this previous iteration, more tanystropheid taxa were found to be unstable by the iterPCR protocol, resulting in a less-inclusive RSCT. *Luxisaurus terrestris* is found as the sister taxon to all remaining tanystropheids in the RSCT, which corresponds to the results of Lu and Liu (2023, note that *Fuyuansaurus acutirostris* was identified as an unstable OTU in the present analysis). The clade composed of the three *Macrocnemus* taxa forms the sister group to all other tanystropheids except *Luxisaurus terrestris*, similar to the result in Spiekman et al. (2024), when not considering the unstable OTUs *Fuyuansaurus acutirostris* and *Augustaburiania vatagini*. The *Tanystropheus* OTUs form a monophyletic group, whereas in Spiekman et al. (2024), *Raibliania calligarisi* was found as the sister taxon to *Tanystropheus longobardicus*. This result was found in 49 out of 52 MPTs of the current analysis, with *Raibliania calligarisi* recovered as the sister taxon to *Ozimek volans* in the remaining three MPTs. As in the analysis of Spiekman et al. (2024), AMNH FARB 7206 and *Tanytrachelos ahynis* form a trichotomy together with the *Tanystropheus* clade in the RSCT. However, whereas *Langobardisaurus pandolfii* was also part of this polytomy in the RSCT of Spiekman et al. (2024), this taxon is here recovered as the sister taxon to the node of this polytomy. *Amotosaurus rotfeldensis* and *Ozimek volans* are sister taxa to each other in the RSCT of Spiekman et al. (2024), but here they are recovered in a polytomy together with the clade that includes *Langobardisaurus pandolfii*, AMNH FARB 7206, *Tanytrachelos ahynis*, and the *Tanystropheus* OTUs in the RSCT.

Trachelosaurus fischeri is found as the sister taxon to the clade composed of *Dinocephalosaurus orientalis* and *Austronaga minuta*, with *Pectodens zhenyuensis* forming the sister taxon to the clade that encompasses these three taxa. Together, these four taxa form Trachelosauridae. Trachelosauridae is defined by the following synapomorphies common to all the MPTs: jugal without posterior process (character 42: 0 → 1), ventral process of postorbital ends much higher than the ventral border of the orbit (character 61: 1 → 0), anterior process of the squamosal continues along the posterior margin of the ventral process of the postorbital and contacts the jugal (character 64: 0 → 1), presence of 11–13 cervical vertebrae (character 195: 1 → 2), mid-dorsal vertebrae with a very wide and "wing-like" transverse process and a distinct connection

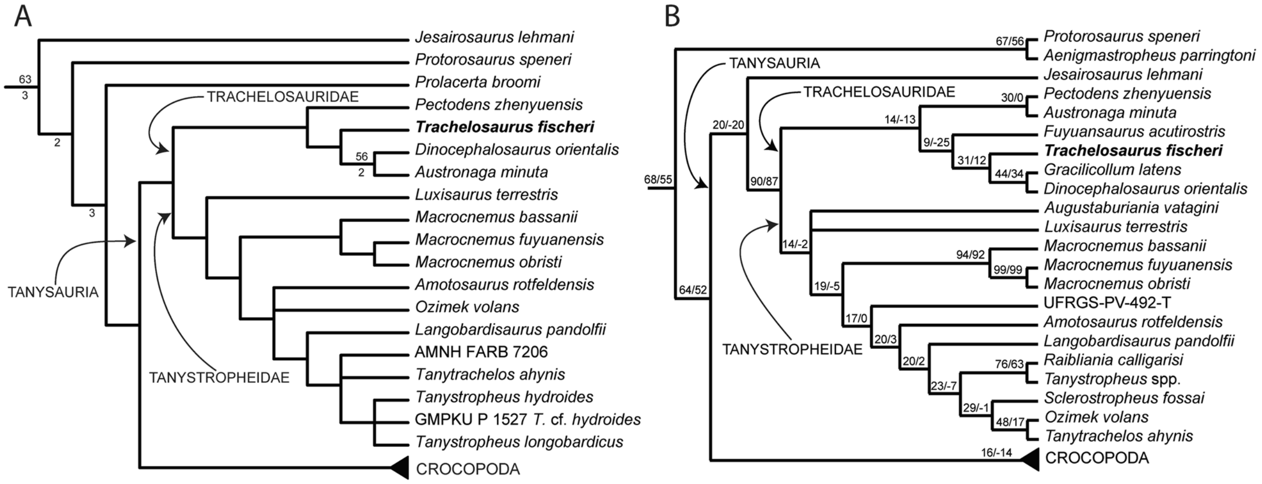

Fig. 10 Results of the phylogenetic analyses. **A** RSCT of all MPTs of the analysis of the Spiekman et al. (2021b) matrix (consistency index: 0.35; retention index: 0.53). Bootstrap GC frequencies >50% are listed above each branch and Bremer supports > 1 are listed below each branch. **B** SCT of all MPTs of all analyses of the CoArTreeP matrix under implied weighting (k values = 19–24). No-zero weight symmetric resampling absolute (left) and GC (right) frequencies are listed above each branch

from the process to the corresponding centrum through a lamina (character 207: 0 → 1), holocephalous anterior dorsal ribs (character 213: 1 → 0), ratio of total length of the humerus versus the total length of the femur between 0.84 and 0.91 (character 248: 1 → 2), astragalus without posterior groove (character 290: 0 → 1), metatarsal V without a hook-shaped proximal end (character 300: 1 → 0), and ratio of length of metatarsal IV versus proximodistal length of metatarsal V between 1.25 and 1.90 (character 305: 1 → 0). The clade comprising *Trachelosaurus fischeri*, *Austronaga minuta*, and *Dinocephalosaurus orientalis* has the following common synapomorphies: more than 13 cervical vertebrae (character 195: 2 → 3), 23 or more dorsal vertebrae (character 204: 0 → 1), ratio of length versus height of the centrum at the level of its posterior articular surface in posterior dorsals between 0.83–1.25 (character 205: 1 → 0), presence of flipper-like limbs (character 239: 0 → 1), ilium without preacetabular process (character 264: 1 → 0), ilium without supra-acetabular crest (character 270: 1 → 0), and femur with linear shaft (character 286: 0 → 1). Finally, *Trachelosaurus fischeri* is defined in all the MPTs by the following autapomorphies: anterior to mid-cervical vertebrae with a spine table (character 180: 0 → 2), cervical ribs short and shaft parallel to the neck (character 199: 2 → 1), and anterior to mid-dorsal vertebrae with gradual transverse expansion of the neural spine (character 203: 0 → 1).

CoArTreeP matrix. The SCT of all the MPTs found in the analyses using the six different concavity constant values ($k = 19-24$) is generally very well resolved, with a few polytomies (see homoplasy indices and fit values in Table 7). This topology is mostly congruent with those of the SCTs found in the analysis 1 of Ezcurra et al. (2023) (in which all analyses were also conducted under implied weighting with $k = 19-24$), and the SCTs of Müller et al. (2023) and Paes-Neto et al. (2023) (these two analyses were conducted only under equal weighting). The only contradictory results are the position of the Long Reef proterosuchian as more closely related to the Erythrosuchidae + Eucrocopoda clade than to Proterosuchidae (contrasting with Ezcurra et al., 2023), the placement of *Tawa hallae* as an herrerasaurian and not as closer to Neotheropoda (contrasting with Ezcurra et al., 2023, but as in Müller et al., 2023), and some aspects of the internal relationships of Tanysauria that are described in detail below.

Trachelosaurus fischeri is recovered in all the MPTs of our analyses within a taxonomically broader Trachelosauridae that is also composed of *Dinocephalosaurus orientalis*, *Gracilicollum latens*, *Fuyuansaurus acutirostris*, *Austronaga minuta*, and *Pectodens zhenyuensis* (Fig. 10B). This group is positioned within a taxonomically larger clade of non-crocopodan archosauromorphs, i.e., Tanysauria, which is also composed of *Jesairosaurus lehmani* and Tanystropheidae. Tanysauria is supported by the following six synapomorphies (character states present in *Trachelosaurus fischeri* indicated with an asterisk, here and below): premaxilla with five or more tooth positions (character 42: 2 → 1*), postorbital-squamosal contact continues ventrally for much or most of the ventral length of the squamosal (character 127: 0 → 1/2), parietal extending over interorbital region (character 160: 0 → 1), interclavicle anterior margin with a median notch (character 407: 0 → 1), humerus with moderate medial

Table 7 Homoplasy indices of the six analyses under implied weighting with the different concavity constant values

Concavity constant value (k)	Consistency index	Retention index	Fit (adjusted homoplasy)
19	0.16844	0.65210	213.30672
20	0.16844	0.65210	205.72592
21	0.16844	0.65210	198.68129
22	0.16844	0.65210	192.11650
23	0.16844	0.65210	185.98298
24	0.16863	0.65256	180.23386

development of the entepicondyle, being poorly projected from the level of the shaft (character 425: 1 → 0), and postfrontal medial margin lateral to parietal (character 832: 0 → 1).

The clade that is composed of Trachelosauridae and Tanystropheidae has the following 12 synapomorphies: maxilla without anterior maxillary foramen (character 52: 1 → 0), maxilla with a separate dorsal apex, forming a distinct process differentiated from the rest of the maxilla by strongly concave or sharply flexed margins (character 58: 0 → 1), postfrontal participating in the border of the supratemporal fenestra (character 123: 0 → 1), axis with anterodorsally expanded neural spine (character 329: 0 → 1), fourth or fifth cervical centrum length versus height of the anterior articular surface greater than 2.92 (character 331: 3/4 → 6/7*), dorsal vertebrae with fan-shaped neural spine in lateral view (character 363: 0 → 1*), scapula and coracoid unfused with each other in non-early juvenile individuals (character 384: 0 → 1), scapula with anterior margin of the blade straight or convex along entire length in lateral view (character 390: 1 → 0), scapula with constriction distal to the glenoid anteroposteriorly longer than half the proximodistal length of the bone (character 391: 1 → 0), humerus with transverse width of the proximal end versus total length of the bone < 0.25 in non-early juvenile individuals (character 416: 1 → 0), ischium with posterior process that extends from the posterodorsal margin (character 488: 0 → 1), and ilium with subtriangular postacetabular process, tapering posteriorly in lateral view (character 688: 0 → 1*).

Five character states are optimised as synapomorphies of Trachelosauridae: premaxilla with anteroposteriorly deep base of the prenarial process (= nasal process) (character 35: 0 → 1*), jugal without posterior process (character 100: 2 → 0), neck with ten or more vertebrae (character 324: 2 → 3*), metatarsal V without a hook-shaped proximal end (character 577: 1 → 0), and axis with postzygapophysis confluent with the neural spine, not protruding posteriorly from the base of the neural spine (character 897: 0 → 1*). *Pectodens zhenyuensis* and *Austronaga minuta* form a clade at the base of Trachelosauridae that is supported by the presence of premaxilla with anteroposterior length of the main body versus its maximum dorsoventral height > 5.00 (character 28: 2 → 4), and jugal with strongly posterodorsally oriented ascending process in an angle equal to or lower than 45° in lateral view when articulated with the maxilla (character 627: 0 → 1). *Fuyuansaurus acutirostris* is recovered as the sister taxon to all other trachelosaurids to the exclusion of the *Pectodens* + *Austronaga* clade, and this group is supported by the presence of anterior-middle and sometimes posterior postaxial cervical vertebrae with distally restricted transverse expansion of the neural spines (not mammillary process) (character 321: 0 → 1*).

Trachelosaurus fischeri is positioned among the more deeply nested trachelosaurids, being the sister taxon to a clade composed of *Dinocephalosaurus orientalis* and *Gracilicollum latens*. The clade that includes *Trachelosaurus fischeri*, *Dinocephalosaurus orientalis*, and *Gracilicollum latens* is supported by the following three synapomorphies: 14 or more cervical vertebrae (character 324: 3 → 4*), ilium without or with incipient preacetabular process (character 460: 1 → 0*), and ilium without supra-acetabular crest (character 667: 1 → 0*). *Dinocephalosaurus orientalis* and *Gracilicollum latens* are found as sister taxa to each other because of the presence of anterior cervical ribs with anterior free-ending process (= accessory process) extending anterior to the prezygapophyses of the corresponding vertebra when in articulation (character 350: 1 → 2).

The base of Tanystropheidae is represented by a trichotomy composed of *Luxisaurus terrestris*, *Augustaburiania vatagini*, and a clade formed by more deeply nested species. *Trachelosaurus fischeri* is excluded from this clade, because it lacks postaxial anterior and middle cervical vertebrae with a distinct longitudinal lamina extending along the lateral surface of the centrum at mid-height (character 340: 0 → 1).

The resampling frequencies are low (< 70%) around the base of Tanysauria, but with a few exceptions. The Trachelosauridae + Tanystropheidae clade has absolute and GC frequencies of 90% and 87%, respectively. Among tanystropheids, high resampling frequencies occur within the genus *Macrocnemus* (> 90%), whereas other frequencies are all lower than 70% to the exclusion of an absolute frequency of 76% for the *Tanystropheus* spp. + *Raibliania calligarisi* clade.

Discussion

Phylogenetic implications

Dinocephalosauridae was erected by Spiekman et al. (2021b) and, based on the analyses therein, was unambiguously composed of *Dinocephalosaurus orientalis* and *Pectodens zhenyuensis*, two taxa known from Member II of the Guanling Formation of Panzhou County, Guizhou Province, in southwestern China. In addition, two specimens, comprising a gravid individual identified as *Dinocephalosaurus* sp. and an isolated embryo, described from the same Member in Luoping County, Yunnan Province, China (Li et al., 2017b; Liu et al., 2017), were considered to represent members of this family (Spiekman et al., 2021b). Recently, *Austronaga minuta*, a small archosauromorph that shares many cranial, cervical, and caudal features with *Dinocephalosaurus orientalis*, was described from the same stratigraphic unit and recovered within Dinocephalosauridae (Wang et al., 2023a), further expanding the known diversity of *Dinocephalosaurus*-like archosauromorphs. In addition, *Gracilicollum latens*, another long-necked archosauromorph from Panzhou County, was recently described and tentatively identified as a tanystropheid (Wang et al., 2023b). However, “dinocephalosaurid” affinities for this taxon were not excluded, and a close affinity with *Dinocephalosaurus orientalis* is indicated by the results of the CoArTreeP matrix here (Fig. 10B; note that *Gracilicollum latens* is identified as an unstable OTU in the analysis of the Spiekman et al., 2021b matrix, but it is recovered among tanystropheids in all MPTs).

The overall morphology of *Trachelosaurus fischeri* is generally very similar to that of *Dinocephalosaurus orientalis* (Spiekman et al., 2024) (Fig. 11). This similarity is also reflected in the results of both phylogenetic analyses, which provide strong support that *Trachelosaurus fischeri* represents a *Dinocephalosaurus*-like archosauromorph (Fig. 10). Specific character states that support the placement of *Trachelosaurus fischeri* among the “dinocephalosaurid” archosauromorphs are the presence of at least 21 cervical vertebrae, at least 27 dorsal vertebrae, very wide and ‘wing-like’ transverse process and a distinct connection between the process and the corresponding centrum through a lamina in mid-dorsal vertebrae, holocephalous anterior dorsal ribs, flipper-like limbs as indicated by the stocky and “simplified” femur with a linear shaft, and the absence of a preacetabular process and supra-acetabular crest on the ilium.

These findings advocate for the inclusion of *Trachelosaurus fischeri* within Dinocephalosauridae Spiekman, Fraser and Scheyer, 2021. However, *Trachelosaurus* already is the type genus of the monotypic Trachelosauridae established by Abel (1919), which has precedence over this taxon. Thus, applying the principle of priority, Dinocephalosauridae Spiekman, Fraser and Scheyer, 2021 should be treated as a junior synonym of Trachelosauridae Abel, 1919 (see Systematic Palaeontology).

Functional morphology

Similar to *Dinocephalosaurus orientalis* (Spiekman et al., 2024), *Trachelosaurus fischeri* possesses an elongate serpentine body composed of a high number of presacral vertebrae and a hyperelongate neck (Fig. 11). It also shares a similar morphology of the ilium, pubis, and femur with *Dinocephalosaurus orientalis*, which lack many features seen in other archosauromorphs (e.g., rounded femoral condyles, a preacetabular process of the ilium, see above). These observations from both the axial and appendicular skeleton, as well as the presence of elongate fangs in the premaxilla that are likely indicative of a piscivorous lifestyle, suggest extensive adaptations to a marine lifestyle in *Trachelosaurus fischeri*. As is hypothesised for *Dinocephalosaurus orientalis* (Spiekman et al., 2024), aquatic propulsion in *Trachelosaurus fischeri* was likely predominantly driven by lateral undulation of its serpentine-like tail and body.

Despite these clear similarities, the axial skeleton of *Trachelosaurus fischeri* also differs from that of *Dinocephalosaurus orientalis* in some noteworthy ways (Fig. 11B), which allows for further functional considerations. With regards to general body proportions, *Trachelosaurus fischeri* likely had a comparatively shorter neck relative to the trunk than *Dinocephalosaurus orientalis*. Furthermore, the dorsal rib shafts of *Trachelosaurus fischeri* possess a distinct, continuously wide curvature, providing the trunk with a barrel-shaped outline in cross-section (Broili & Fischer, 1918; Fig. 11A). However, the most important distinction is the unique morphology of the cervical ribs in *Trachelosaurus fischeri*, which barely extend beyond the length of the corresponding vertebra and are relatively stocky and posteriorly bifurcated in lateral view (Fig. 6B). This is in marked contrast to all other tanysaurians, in which the cervical ribs are thin and elongate, extending the length of several cervical vertebrae (Spiekman et al., 2021b). In the long-necked aquatic archosauromorphs *Tanystropheus* spp., *Dinocephalosaurus orientalis*, and *Gracilicollum latens*, the cervical ribs are even more elongated relative to body size than in other archosauromorphs. In the latter two taxa, they span the length of up to five or six intervertebral articulations (Spiekman et al., 2024; Wang et al., 2023b). It has been hypothesised that this elongation of the cervical ribs was a prerequisite for the extreme elongation of the neck in *Tanystropheus* spp., where the overlapping cervical ribs would form a stiffened bundle that provided support to the extremely elongated and slender cervical column (Jaquier & Scheyer, 2017; Tschanz, 1986). The necks of

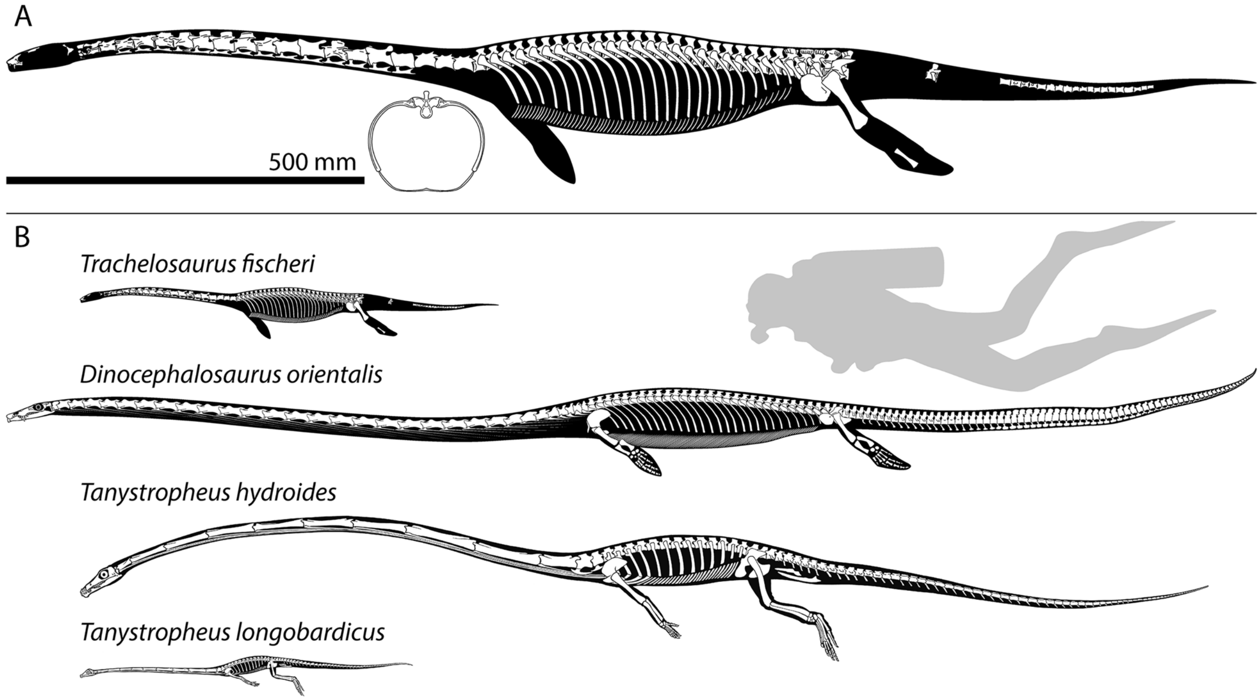

Fig. 11 Skeletal reconstruction of *Trachelosaurus fischeri* and comparison with other long-necked, aquatic tanysaurians. **A** Skeletal reconstruction and interpretive silhouette of *Trachelosaurus fischeri* in left lateral view and anteroposterior view of the mid-anterior portion of the torso (reconstructions by E. M.); based on the elements preserved on MLU.GeoS.1612. **B** Comparison of *Trachelosaurus fischeri* with *Dinocephalosaurus orientalis* (from Spiekman et al., 2024; reconstruction by S. N. F. S.), *Tanystropheus hydroides,* and *Tanystropheus longobardicus* (both from Spiekman et al., 2020a; reconstructions by Beat Scheffold); the outline of a 170-cm-tall human in scuba diving equipment is used to indicate the scale

Dinocephalosaurus orientalis and *Gracilicollum latens* are composed of considerably more cervical vertebrae that are less elongated than in *Tanystropheus* spp. (Wang et al., 2023b). They thus represent a distinctly different cervical configuration (Fig. 11B), which evolved independently from that of *Tanystropheus* spp. (Spiekman et al., 2021b, 2024; Wang et al., 2023b), and although it is generally accepted that the neck of *Tanystropheus* spp. was relatively stiffened (e.g., Nosotti, 2007; Tschanz, 1986), the range of movement and the influence of the extremely elongated cervical ribs remain unclear for *Dinocephalosaurus orientalis* and *Gracilicollum latens*. The presence of the short and morphologically unique cervical ribs of *Trachelosaurus fischeri* combined with an otherwise broadly similar configuration of the cervical column to *Dinocephalosaurus orientalis* and *Gracilicollum latens* clearly shows that overlapping, extremely elongated cervical ribs were not a necessity to support such an elongate neck in water in these taxa. Despite this observation, the exact function of the unique cervical ribs of *Trachelosaurus fischeri* and their bifurcation remains unclear.

Posteriorly bifurcated postaxial cervical rib shafts also occur among dinosaurs in abelisaurid theropods, ceratopsians, and sauropods (Bonaparte et al., 1990; O'Connor, 2007; Xu et al., 2010; Wedel & Taylor, 2023). The bifurcated shafts of abelisaurid theropods are distinctly asymmetric, with a longer and thinner 'styliform' ventral process that has been hypothesised to represent an ossified tendon of cervical musculature (e.g., *M. longus colli lateralis*) (O'Connor, 2007). Among ceratopsians, the bifurcation is less distinct and formed by a 'prominent accessory dorsal process' of the rib shaft (Xu et al., 2010). In sauropods, bifurcations of the cervical ribs occur in some turiasaurian and diplodocid taxa to various degrees. It has been hypothesised that these bifurcations in sauropods are related to the attachment of cervical musculature (i.e., *M. flexor colli lateralis* and *M. longus colli ventralis*) that flex in opposing directions (Wedel & Taylor, 2023). It was suggested that the rib shaft bifurcation might have improved muscular control of the middle portion of the neck by optimising muscle insertion angles. It is striking that the cervical ribs with bifurcating shafts are comparatively short in length for sauropod cervical ribs, and that the cervical ribs of *Trachelosaurus fischeri* are also drastically shorter than those of other tanysaurians. Nevertheless, a homologous functional interpretation of the rib shaft bifurcation between sauropods and *Trachelosaurus fischeri* cannot be assumed, and evidence for muscle insertion sites on the cervical ribs is not conclusive in MLU.GeoS.1612. Furthermore, the bifurcation of the cervical ribs is considerably more prominent in *Trachelosaurus fischeri* than that in the above-mentioned dinosaur groups, and this bifurcation is consistent throughout at least most of the cervical series, whereas in dinosaurs, the presence and morphology of the bifurcation is strongly variable throughout the cervical series within individuals.

The shape of the neural spines of both the cervical and dorsal vertebrae in *Trachelosaurus fischeri* also differs from that seen in *Tanystropheus* spp., *Dinocephalosaurus orientalis*, and *Gracilicollum latens*. The neural spines of the cervical vertebrae in *Dinocephalosaurus orientalis* are low and possess a distal margin that is concave in lateral view (Spiekman et al., 2024). This condition is even more distinct in *Tanystropheus* spp., in which the neural spine in the mid-cervical vertebrae is reduced to small dorsal extensions of the neural arch near the anterior and posterior ends of the vertebra (Spiekman & Scheyer, 2019; Wild, 1973). It has been suggested that this reduction of the cervical neural spines corresponds to a reduced attachment area for the adductor musculature of the neck, and correspondingly, that dorsiflexion of the neck was limited in these taxa (Tschanz, 1986, 1988; but see Renesto, 2005). *Gracilicollum latens*, in contrast, has comparatively taller cervical neural spines with a straight distal margin in lateral view that also possesses a slight transverse expansion (Wang et al., 2023b). This configuration corresponds closely with that seen in tanysaurians with less elongated necks and likely terrestrial habits, such as *Macrocnemus* spp., *Fuyuansaurus acutirostris*, and *Langobardisaurus pandolfii* (Fraser et al., 2013; Renesto, 1994; Scheyer et al., 2020).

The condition of *Trachelosaurus fischeri* deviates from all above-mentioned taxa in possessing neural spines with a distal end that is slightly convex in lateral view (Fig. 6C). Among non-crocopodan archosauromorphs, this condition is also found in *Protorosaurus speneri*, *Prolacerta broomi*, *Jesairosaurus lehmani*, and the posterior cervical vertebrae of *Tanystropheus "conspicuus"* (Wang et al., 2023b; pers. Obs. A. R.). In addition, a distinct transverse expansion of the distal end of the neural spines accompanied by strongly rugose patterning is present in *Trachelosaurus fischeri* in both the cervical and dorsal vertebrae, with this condition being most extensive in the latter region of the column (Figs. 6C, 7B, D). This degree of transverse expansion of the distal end of the cervical neural spines is absent in other known tanystropheids and trachelosaurids, but present to some extent in the dorsal vertebrae of several taxa, including *Tanystropheus* spp. and *Dinocephalosaurus orientalis* (Spiekman et al., 2021b). In *Dinocephalosaurus orientalis*, this expansion is also accompanied by rugosities, but to a considerably lesser extent than in *Trachelosaurus fischeri* (Spiekman et al., 2024). It was previously suggested that the distally expanded dorsal neural spines in *Tanystropheus* spp. supported a supraspinous ligament system that would have stiffened the trunk to the extent that it would have severely limited lateral undulation of the body (Renesto & Saller, 2018). However, this interpretation was not supported quantitatively, and it was deemed unlikely by Spiekman et al. (2020b), who saw no clearly supported limitations to lateral undulation in *Tanystropheus hydroides* based on comparisons to other laterally undulating reptile taxa. Both *Dinocephalosaurus orientalis* and *Trachelosaurus fischeri* exhibit more extensive distal expansions of the dorsal neural spines, accompanied by rugosities, and it seems plausible that both taxa would have possessed more extensive supraspinous ligaments than *Tanystropheus* spp. (Spiekman et al., 2024; see also the wide transverse expansions of the neural spines in the Hayden Quarry tanystropheid material and associated discussion on ligaments in Pritchard et al., 2015). Nevertheless, it seems highly unlikely that the very long dorsal vertebral column in these taxa would have been stiffened to such a degree that it precluded lateral undulation as a means of propulsion, also when considering the relative length of the limbs compared to the elongate axial column in *Dinocephalosaurus orientalis* (Spiekman et al., 2024). Instead, the large number of dorsal vertebrae likely increased the flexibility of the trunk in *Dinocephalosaurus orientalis* and *Trachelosaurus fischeri*. This interpretation is supported by IVPP V20295, the most complete *Dinocephalosaurus orientalis* specimen, which exhibits extensive dorsiflexion of the vertebral column (= opisthotonus, see Faux & Padian, 2007) to the extent that the entire axial column forms two complete spirals throughout its length (Spiekman et al., 2024). This flexure is considerably more pronounced in the dorsal region than in the cervical or caudal regions, suggesting considerable flexibility of the torso, at least in a dorsal direction. Supraspinous ligaments might have provided much needed strengthening to support such an elongate presacral column without functionally restricting lateral undulation in these taxa.

Palaeoenvironmental and biogeographical implications

MLU.GeoS.1612 was found in a platy sandstone that also contains relatively small tetrapod tracks (Broili & Fischer, 1918; Fig. 2B, H), which indicates that the rock unit falls within the Thüringischer Chirotheriensandstein (Klein, 2021). This unit forms the top of the Solling Formation (Bachmann et al., 2021; Fig. 1). The occurrence of tetrapod footprints is in line with sedimentological data on a coastal origin of the sandstones, and the shallow marine environment of these track-rich rocks (including abundant chirotheriids) has been concluded from a range of further sedimentary features (Hauschke et al., 2005; Puff & Radzinski, 1980). It is important not to confuse the platy fine-grained sandstones that contain the tracks and *Trachelosaurus fischeri* with the more massive and coarse-grained sandstones that produced numerous temnospondyl remains (Schoch, 2018, 2019). The latter were derived from more basal layers in the lower Solling Formation dated as late Olenekian (Spathian) (Bachmann et al., 2021).

The occurrence of *Trachelosaurus fischeri* in a coastal-to-shallow marine environment and its close relationship to the fully marine *Dincephalosaurus orientalis* both indicate that the taxon probably was a euhaline reptile that dwelled the riparian zone of the Röt Sea in the earliest Anisian (Aegean). The presence of tetrapod footprints together with the potential desiccation structures suggests that the carcass of this individual was most likely washed into an intertidal area, with recurrent subaerial exposition and evaporation.

Trachelosaurus fischeri is both the first recognised European trachelosaurid and the oldest known trachelosaurid (earliest Anisian) globally, with other members of this clade so far having been found only in the Guanling Formation of China (Pelsonian, middle Anisian; Wang et al., 2014). Recently, it was shown that the remains of the enigmatic reptile (cf.) *Lamprosauroides goepperti* (*nomen dubium*), consisting of isolated maxillae and a hemimandible, were morphologically very similar to *Dinocephalosaurus orientalis* (Spiekman et al., 2024). *Lamprosauroides* is known from the Lower Muschelkalk of Upper Silesia, Poland, and possibly Winterswijk, The Netherlands (Spiekman & Klein, 2021), and it is roughly contemporaneous with *Trachelosaurus fischeri*. Although this material is still insufficient for a confident taxonomic identification, the presence of trachelosaurids in the Central European Basin during the earliest Anisian makes the similarity between *Lamprosauroides goepperti* and *Dinocephalosaurus orientalis* particularly intriguing.

Conclusion

Trachelosaurus fischeri is a marine reptile that is known from a single specimen from the Middle Buntsandstein of the Solling Formation (early Anisian, Middle Triassic), near Bernburg an der Saale in Saxony-Anhalt, Germany. The specimen consists of a mostly disarticulated skeleton, including most of the presacral vertebrae, two sacral vertebrae, several caudal vertebrae, part of the pelvis and hind limb, and some limited skull remains (Fig. 11A). The slabs containing the specimen also preserve numerous tetrapod footprints and the depositional environment corresponds to an intertidal marine setting.

We provide a detailed redescription of this historical specimen, and find that it represents a marine archosauromorph with a high presacral vertebral count (at least 21 cervical and 27 dorsal vertebrae). *Trachelosaurus fischeri* differs from other known early archosauromorphs in possessing relatively short cervical ribs with a bifurcating shaft and presacral vertebrae with a strong transverse distal expansion of the neural spines, accompanied by extensive rugosities, possibly indicative of a supraspinous ligamental system. The limited remains of the appendicular skeleton, including an ilium that lacks a preacetabular process and a stocky, straight femur, are indicative of flipper-like limbs, similar to *Dinocephalosaurus orientalis* (Spiekman et al., 2024). Similar to this taxon, lateral undulation of its tail and elongated body likely represented the main mode of aquatic propulsion for *Trachelosaurus fischeri*.

The results of our phylogenetic analyses (Fig. 10), conducted using two separate data matrices that sample most of the known diversity of non-archosauriform archosaurmorphs, show strong support that *Trachelosaurus fischeri* is closely related to *Dinocephalosaurus orientalis*, and both are recovered within a clade that excludes tanystropheids. This clade was previously identified as Dinocephalosauridae Spiekman, Fraser and Scheyer, 2021, but the inclusion of *Trachelosaurus fischeri* implies that Trachelosauridae Abel, 1919 is its senior synonym. *Trachelosaurus fischeri* currently represents the oldest known trachelosaurid and the first unambiguously identified member of this family outside the Guanling Formation of China. Furthermore, our phylogenetic results corroborate previous findings (e.g., Spiekman et al., 2021b) that trachelosaurids and tanystropheids form a monophyletic group that excludes *Protorosaurus speneri* and *Prolacerta broomi*, thus not representing a monophyletic "Protorosauria" or "Prolacertiformes". This clade of particularly long-necked archosauromorphs is named Tanysauria clade nov. and represents the sister group to Crocopoda. We also propose an emended definition of Tanystropheidae Camp, 1945 based on the above-mentioned findings.

The identification of *Trachelosaurus fischeri* as a *Dinocephalosaurus*-like archosauromorph with extensive aquatic adaptations, a high presacral vertebral count, and an elongate neck, adds to the growing evidence for the presence during the Middle Triassic of a diverse group of fully marine, long-necked archosauromorphs positioned within Trachelosauridae. This group additionally includes *Dinocephalosaurus orientalis* and an unnamed trachelosaurid embryo, as well as possibly *Austronaga minuta* and *Gracilicollum latens* (Li et al., 2017b; Spiekman et al., 2024; Wang et al., 2023a, 2023b), with *Pectodens zhenyuensis* and potentially *Fuyuansaurus acutirostris* as more terrestrial sister taxa (Fraser et al., 2013; Li et al., 2017a). This group is remarkable in its apparent degree of adaptations to marine habits, which among all of Archosauromorpha otherwise only occurred among metriorhynchid crocodylomorphs, as well as in its similarity to long-necked Jurassic and Cretaceous plesiosaurs through the presence of elongate necks and flipper-like limbs.

Supplementary Information

The online version contains supplementary material available at https://doi.org/10.1186/s13358-024-00309-6.

Additional file 1: Supplementary files related to the phylogenetic analyses of the Spiekman et al. (2021) matrix.

Additional file 2: Supplementary files related to the phylogenetic analyses of the CoArTreeP matrix

Acknowledgements
The authors are grateful to Maximilian Albrecht (MLU) for specimen access and discussions. Feiko Miedema, Erin Maxwell (both SMNS), Nick Fraser (National Museums Scotland), and Torsten Scheyer (University of Zurich) are thanked for discussions. The authors acknowledge the Willi Hennig Society for making TNT freely available. This study used computational resources from Universidad Nacional de Córdoba (https://ccad.unc.edu.ar/), which are part of SNCAD–MinCyT, Argentina. Two anonymous reviewers and editors Nicole Klein and Daniel Marty are thanked for constructive comments that helped to improve the manuscript.

Author contributions

Conceptualization: SNFS, MDE, MB, and RRS. Methodology: SNFS and MDE. Investigation: SNFS, MDE, WW, AR, and EM. Visualisation: SNFS, MDE, and EM. Writing—original draft: SNFS, MDE, AR, EM, and RRS. Writing—review and editing: SNFS, MDE, AR, WW, EM, MB, and RRS.

Funding
SNFS is funded by the Deutsche Forschungsgemeinschaft (Grant No. SCHO 791/7–1 to RRS). MDE is funded by the Agencia Nacional de Promoción Científica y Tecnológica (Grant No. PICT 2018–01186).

Availability of data and materials

All data generated or analysed during this study are included in this published article and its additional information files

Declarations

Competing interests

The authors declare no competing interests.

Author details
[1]Staatliches Museum für Naturkunde Stuttgart, Rosenstein 1, 70191 Stuttgart, Germany. [2]Sección Paleontología de Vertebrados, CONICET–Museo Argentino de Ciencias Naturales "Bernardino Rivadavia", Ángel Gallardo 470, C1405DJR Ciudad Autónoma de Buenos Aires, Argentina. [3]Institute of Paleobiology, Polish Academy of Sciences, Twarda 51/55, 00-818 Warsaw, Poland. [4]Key Laboratory of Vertebrate Evolution and Human Origins of Chinese Academy of Sciences, Institute of Vertebrate Paleontology and Paleoanthropology, Chinese Academy of Sciences, Beijing, China. [5]Institut Català de Paleontologia Miquel Crusafont (ICP-CERCA), Universitat Autònoma de Barcelona, Edifici ICTA-ICP, c/Columnes s/n, Campus de la UAB, 08193 Cerdanyola del Vallès, Barcelona, Spain. [6]Museum für Naturkunde Magdeburg, Magdeburg, Germany. [7]Fachgebiet Paläontologie, Institut für Biologie, Universität Hohenheim, 70599 Stuttgart, Germany.

Received: 10 November 2023 Accepted: 2 February 2024

References

Abel, O. (1919). *Die Stämme der Wirbeltiere*. W de Gruyter.

Abel, O. (1920). *Lehrbuch der Paläozoologie*. Gustav Fischer.

Appleby, R., Charig, A., Cox, C., Kermack, K., & Tarlo, L. B. (1967). Reptilia. In W. Harland, C. Holland, M. House, N. Hughes, A. Reynolds, M. Rudwick, G. Satterthwaite, L. B. Tarlo, & E. Willey (Eds.), *The fossil record. Part II*. Geological Society.

Arthaber, G. (1924). Die Phylogenie der Nothosaurier. *Acta Zoologica, 5*, 441–516.

Bachmann, G. H., Franz, M., & Kozur, H. W. (2021). Korrelation der Germanischen Trias mit der internationalen Gliederung. In N. Hauschke, M. Franz, & G. H. Bachmann (Eds.), *Trias. Aufbruch ins Erdmittelalter* (pp. 40–48). Pfeil: Munich.

Bassani, F. (1886). Sui fossili e sull'eta degli schisti bituminosi triasici di Besano in Lombardia. *Atti Società Italiana di scienze naturali*, *29*, 15–72.

Benton, M. J., & Allen, J. L. (1997). *Boreopricea* from the Lower Triassic of Russia, and the relationships of the prolacertiform reptiles. *Palaeontology, 40*(4), 931–953.

Berliner, A., & Pütter, A. (1917). Geologische Mitteilungen. *Die Naturwissenschaften, 5*(52), 766–768.

Bertin, T. J. C., Thivichon-Prince, B., LeBlanc, A. R. H., Caldwell, M. W., & Viriot, L. (2018). Current perspectives on tooth implantation, attachment, and replacement in Amniota. *Frontiers in Physiology*. https://doi.org/10.3389/fphys.2018.01630

Bonaparte, J. F., Novas, F. E., & Coria, R. A. (1990). *Carnotaurus sastrei* Bonaparte, the horned, lightly built carnosaur from the Middle Cretaceous of Patagonia. *Contributions in Science, Natural History Museum of Los Angeles County, 416*, 1–41.

Borsuk-Białynicka, M., & Evans, S. E. (2009). A long-necked archosauromorph from the Early Triassic of Poland. *Palaeontologia Polonica, 65*, 203–234.

Borsuk-Białynicka, M., Cook, E., Evans, S. E., & Maryańska, T. (1999). A microvertebrate assemblage from the Early Triassic of Poland. *Acta Palaeontologica Polonica, 44*(2), 167–188.

Broili, F., & Fischer, E. (1918). *Trachelosaurus fischeri* nov. gen. nov. sp. Ein neuer Saurier aus dem Buntsandstein von Bernburg. *Jahrbuch Der Königlich Preussischen Geologischen Landesanstalt Zu Berlin, 37*(1), 359–414.

Broom, R. (1903). On a new reptile (Proterosuchus fergusi) from the Karoo beds of Tarkastad, South Africa. *Annals of the South African Museum*, *4*, 158–164.

Buchwitz, M., Marchetti, L., Jansen, M., Falk, D., Trostheide, F., & Schneider, J. W. (2020). *Ichnotaxonomy and trackmaker assignment of tetrapod tracks and swimming traces from the Middle Permian Hornburg Formation of Saxony-Anhalt (Germany)*. Paper presented at the Annales Societatis Geologorum Poloniae.

Butler, R. J., Ezcurra, M. D., Liu, J., Sookias, R. B., & Sullivan, C. (2019). The anatomy and phylogenetic position of the erythrosuchid archosauriform *Guchengosuchus shiguaiensis* from the earliest Middle Triassic of China. *PeerJ, 7*, e6435. https://doi.org/10.7717/peerj.6435

Camp, C. L. (1945). *Prolacerta* and the protorosaurian reptiles. Part 1. *American Journal of Science, 243*, 1732.

Carroll, R. L. (1969). A Middle Pennsylvanian captorhinomorph, and the interrelationships of primitive reptiles. *Journal of Paleontology, 43*(1), 151–170.

Carroll, R. L. (1981). Plesiosaur ancestors from the Upper Permian of Madagascar. *Philosophical Transactions of the Royal Society of London. b, Biological Sciences, 293*(1066), 315–383. https://doi.org/10.1098/rstb.1981.0079

Carroll, R. L. (1988). *Vertebrate paleontology and evolution*. W. H. Freeman and Company.

Chen, X.-H., Motani, R., Cheng, L., Jiang, D.-Y., & Rieppel, O. (2014). The enigmatic marine reptile *Nanchangosaurus* from the Lower Triassic of Hubei, China and the phylogenetic affinities of Hupehsuchia. *PLoS ONE, 9*(7), e102361. https://doi.org/10.1371/journal.pone.0102361

Cossmann, M. (1922). Reptiles et Mammiféres. *Revue Critique De Paléozoologie Et De Paléophytologie, 26*(3), 90–96.

Dilkes, D. W. (1998). The Early Triassic rhynchosaur *Mesosuchus browni* and the interrelationships of basal archosauromorph reptiles. *Philosophical Transactions of the Royal Society of London B: Biological Sciences, 353*, 501–541. https://doi.org/10.1098/rstb.1998.0225

Dzik, J., & Sulej, T. (2016). An early Late Triassic long-necked reptile with a bony pectoral shield and gracile appendages. *Acta Palaeontologica Polonica, 61*(4), 805–823. https://doi.org/10.4202/app.00276.2016

Edinger, T. (1921). Über *Nothosaurus* II. Zur Gaumenfrage. *Senckenbergiana*, (1920)(3), 193–205.

Evans, S. E. (1988). The early history and relationships of the Diapsida. *In The Phylogeny and Classification of the Tetrapods, Volume 1: Amphibians. Reptiles, Birds, by Benton, M J, Clarendon Press, Oxford, Systematics Association Special Volume No., 35A*, 221–260.

Ezcurra, M. D. (2016). The phylogenetic relationships of basal archosauromorphs, with an emphasis on the systematics of proterosuchian archosauriforms. *PeerJ, 4*, e1778. https://doi.org/10.7717/peerj.1778

Ezcurra, M. D. (2023). Exploring different weightings against homoplasy in genealogies of paleontological phylogenetic matrices. *Abstract Book Annual Meeting of the Willi Hennig Society XL: 8*.

Ezcurra, M. D., Bandyopadhyay, S., & Sen, K. (2022). A new faunistic component of the Lower Triassic Panchet Formation of India increases the continental non-archosauromorph neodiapsid record in the aftermath of the end-Permian mass extinction. *Journal of Paleontology, 96*(2), 428–438. https://doi.org/10.1017/jpa.2021.100

Ezcurra, M. D., Bandyopadhyay, S., Sengupta, D. P., Sen, K., Sennikov, A. G., Sookias, R. B., Nesbitt, S. J., & Butler, R. J. (2023). A new archosauriform species from the Panchet Formation of India and the diversification of Proterosuchidae after the end-Permian mass extinction. *Royal Society Open Science, 10*, 230387. https://doi.org/10.1098/rsos.230387

Ezcurra, M. D., & Butler, R. J. (2018). The rise of the ruling reptiles and ecosystem recovery from the Permo-Triassic mass extinction. *Proceedings of the Royal Society B: Biological Sciences, 285*, 20180361. https://doi.org/10.1098/rspb.2018.0361

Ezcurra, M. D., Scheyer, T. M., & Butler, R. J. (2014). The origin and early evolution of Sauria: Reassessing the Permian saurian fossil record and the timing of the crocodile-lizard divergence. *PLoS ONE, 9*(2), e89165. https://doi.org/10.1371/journal.pone.0089165

Ezcurra, M. D., Fiorelli, L. E., Martinelli, A. G., Rocher, S., von Baczko, M. B., Ezpeleta, M., Taborda, J. R. A., Hechenleitner, E. M., Trotteyn, M. J., & Desojo, J. B. (2017). Deep faunistic turnovers preceded the rise of dinosaurs in southwestern Pangaea. *Nature Ecology & Evolution, 1*, 1477–1483. https://doi.org/10.1038/s41559-017-0305-5

Ezcurra, M. D., & Sues, H.-D. (2022). A re-assessment of the osteology and phylogenetic relationships of the enigmatic, large-headed reptile *Sphodrosaurus pennsylvanicus* (Late Triassic, Pennsylvania, USA) indicates archosauriform affinities. *Journal of Systematic Palaeontology*. https://doi.org/10.1080/14772019.2022.2057820

Faux, C. M., & Padian, K. (2007). The opisthotonic posture of vertebrate skeletons: Postmortem contraction or death throes? *Paleobiology, 33*(2), 201–226. https://doi.org/10.1666/06015.1

Flynn, J. J., Nesbitt, S. J., Michael Parrish, J., Ranivoharimanana, L., & Wyss, A. R. (2010). A new species of Azendohsaurus (Diapsida: Archosauromorpha) from the Triassic Isalo Group of southwestern Madagascar: cranium and mandible. *Palaeontology*, *53(3)*, 669–688. https://doi.org/10.1111/j.1475-4983.2010.00954.x

Foth, C., Ezcurra, M. D., Sookias, R. B., Brusatte, S. L., & Butler, R. J. (2016). Unappreciated diversification of stem archosaurs during the Middle Triassic predated the dominance of dinosaurs. *BMC Evolutionary Biology, 16*(1), 188. https://doi.org/10.1186/s12862-016-0761-6

Fraser, N. C., Rieppel, O., & Li, C. (2013). A long-snouted protorosaur from the Middle Triassic of southern China. *Journal of Vertebrate Paleontology, 33*(5), 1120–1126. https://doi.org/10.1080/02724634.2013.764310

Gadow, H. (1933). *The evolution of vertebral column*. Cambridge University Press.

Goloboff, P. A. (1999). Analyzing large data sets in reasonable times: Solutions for composite optima. *Cladistics, 15*(4), 415–428. https://doi.org/10.1006/clad.1999.0122

Goloboff, P. A., & Morales, M. E. (2023). TNT version 1.6, with a graphical interface for MacOS and Linux, including new routines in parallel. *Cladistics, 39*(2), 144–153. https://doi.org/10.1111/cla.12524

Goloboff, P. A., Farris, J. S., Källersjö, M., Oxelman, B., Ramırez, M. N. J., & Szumik, C. A. (2003). Improvements to resampling measures of group support. *Cladistics, 19*(4), 324–332. https://doi.org/10.1111/j.1096-0031.2003.tb00376.x

Gottmann-Quesada, A., & Sander, P. M. (2009). A redescription of the early archosauromorph *Protorosaurus speneri* Meyer, 1832, and its phylogenetic relationships. *Paleontographica, 287*, 123–220. https://doi.org/10.1127/pala/287/2009/123

Gow, C. E. (1975). The morphology and relationships of *Youngina capensis* Broom and *Prolacerta broomi* Parrington. *Palaeontologica Africana, 18*, 89–131.

Griffin, C. T., Stocker, M. R., Colleary, C., Stefanic, C. M., Lessner, E. J., Riegler, M., Formoso, K., Koeller, K., & Nesbitt, S. J. (2021). Assessing ontogenetic maturity in extinct saurian reptiles. *Biological Reviews, 96*(2), 470–525. https://doi.org/10.1111/brv.12666

Haubold, H. (1971). Die Tetrapodenfährten des Buntsandsteins in der Deutschen Demokratischen Republik und in Westdeutschland und ihre Äquivalente in der gesamten Trias. *Paläontologische Abhandlungen, A, 4*, 397–548.

Hauschke, N. (2018). *Chapter 26. HALLE: The Palaeontological Collection of the Martin Luther University Halle-Wittenberg in Halle (Saale).* In L. A. Beck & U. Joger (Eds.), Paleontological Collections of Germany, Austria and Switzerland. The History of Life of Fossil Organisms at Museums and Universities (pp. 281–292). Springer.

Hauschke, N., Franz, M., & Bachmann, G. H. (2021). *Trias. Aufbruch in das Erdmittelalter.* Dr. Friedrich Pfeil.

Hauschke, N., & Mertmann, D. (2015). Ausgewählte Fossilfunde aus den Geologisch-Paläontologischen Sammlungen der Martin-Luther-Universität in Halle (Saale): Sachsen-Anhalt. *Der Aufschluss, 66*, 335–351.

Hauschke, N., Shukla, U., & Becker, A. (2005). Der Chirotheriensandstein (Solling-Formation, Mittlerer Buntsandstein) im Merkelschen Steinbruch in Bernburg an der Saale (Sachsen-Anhalt)—neue Untersuchungen in einem klassischen Aufschluss. *Hallesches Jahrbuch für Geowissenschaften(B), 19*, 95–108.

Hone, D. W. E., & Benton, M. J. (2008). Contrasting supertree and total-evidence methods: The origin of the pterosaurs. *Zitteliana, 28*, 35–60.

Huene, F. R. (1902). Übersicht über die Reptilien der Trias. *Geologische Und Paläontologische Abhandlungen (neue Serie), 6*, 1–84.

Huene, F. R. (1944). Über die systematische Stellung von *Trachelosaurus* aus dem Buntsandstein von Bernburg. *Neues Jahrbuch Für Mineralogie, Geologie Und Paläontologie, Monatshefte, Abteilung B, 6*, 170–174.

Huene, F. R. (1948). Short review of the lower tetrapods. In A. L. Du Toit (Ed.), *Robert Broom commemorative volume. Special publication of the royal society of South Africa.* Cape Town, South Africa: Galvin & Sales.

Huene, F. R. (1954). Ein neuer Protorosauridae. *Neues Jahrbuch Fur Geologie Und Palaontologie, Monatshefte, 5*, 228–230.

Huene, F. R. (1956). *Paläontologie und Phylogenie der niederen Tetrapoden*. Fischer.

International Commission on Zoological Nomenclature. (1998). *Nothosaurus* Münster, 1834 (Reptilia, Sauropterygia): Given precedence over *Conchiosaurus* Meyer, (1833). *Bulletin of Zoological Nomenclature, 55*(3), 197–198.

Jalil, N.-E. (1997). A new prolacertiform diapsid from the Triassic of North Africa and the interrelationships of the Prolacertiformes. *Journal of Vertebrate Paleontology, 17*(3), 506–525. https://doi.org/10.1080/02724634.1997.10010998

Jaquier, V. P., Fraser, N. C., Furrer, H., & Scheyer, T. M. (2017). Osteology of a new specimen of *Macrocnemus* aff. *M. fuyuanensis* (Archosauromorpha, Protorosauria) from the Middle Triassic of Europe: Potential implications for species recognition and paleogeography of tanystropheid protorosaurs. *Frontiers in Earth Science, 5*(91), 1–28. https://doi.org/10.3389/feart.2017.00091

Jaquier, V. P., & Scheyer, T. M. (2017). Bone histology of the Middle Triassic long-necked reptiles *Tanystropheus* and *Macrocnemus* (Archosauromorpha, Protorosauria). *Journal of Vertebrate Paleontology, 37*(2), e1296456. https://doi.org/10.1080/02724634.2017.1296456

Klein, H. (2021). Tetrapodenfährten der Germanischen Trias Mitteleuropas und angrenzender Gebiete. In N. Hauschke, M. Franz, & G. H. Bachmann (Eds.), *Trias. Aufbruch ins Erdmittelalter* (Vol. 1, pp. 349–356). Munich: Pfeil.

Kuhn, O. (1935). *Fossilium Catalogus. I: Animalia. Part 69. Sauropterygia* (W. Quenstedt (ed.)). W. Junk.

Kuhn, O. (1960). Die Familien der fossilen Amphibien und Reptilien. *Bericht Der Naturforschenden Gesellschaft Bamberg, 37*, 20–52.

Kuhn, O. (1961a). *Die Familien der rezenten und fossilen Amphibien und Reptilien*. Verlagshaus Meisenbach KG.

Kuhn, O. (1961b). *Fossilium Catalogus. I: Animalia. Pars 99. Reptilia (Supplementum 1(2))* (F. Westphal (ed.)). W. Junk.

Kuhn, O. (1963). *Fossilium Catalogus. I: Animalia. Part 104. Sauria (Supplementum I)* (F. Westphal (ed.)). W. Junk.

Kuhn, O. (1971). *Die Saurier der Deutschen Trias*. Geiselberger.

Kuhn, O. (1975). Die deutschen Saurier, Nachtrag II. *Bericht Der Naturforschenden Gesellschaft Bamberg, 50*, 5–23.

Lang, M., & von Huene, F. (1952). *Die Saurier Thüringens nach Erhebungen ihres centralen Betreuerns Hugo Rühle von Lilienstern*. G. Fischer.

Li, C. (2003). First record of protorosaurid reptile (Order Protorosauria) from the Middle Triassic of China. *Acta Geologica Sinica, 77*(4), 419–423. https://doi.org/10.1111/j.1755-6724.2003.tb00122.x

Li, C., Fraser, N. C., Rieppel, O., Zhao, L.-J., & Wang, L.-T. (2017a). A new diapsid from the Middle Triassic of southern China. *Journal of Paleontology, 91*, 1306–1312. https://doi.org/10.1017/jpa.2017.12

Li, C., Rieppel, O., & Fraser, N. C. (2017b). Viviparity in a Triassic marine archosauromorph reptile. *Vertebrata PalAsiatica, 55*(3), 210–217.

Liu, J., Organ, C. L., Benton, M. J., Brandley, M. C., & Aitchison, J. C. (2017). Live birth in an archosauromorph reptile. *Nature Communications, 8*, 14445. https://doi.org/10.1038/ncomms14445

Lu, Y.-T., & Liu, J. (2023). A new tanystropheid (Diapsida: Archosauromorpha) from the Middle Triassic of SW China and the biogeographical origin of Tanystropheidae. *Journal of Systematic Palaeontology, 21*(1), 2250778. https://doi.org/10.1080/14772019.2023.2250778

Mader, D. (1982). Genese des mitteleuropäischen Buntsandsteins—Entwicklungsgeschichte einer kontinentalen Rotformation. *Naturwissenschaften, 69*, 311–325. https://doi.org/10.1007/BF00480451

Meyer, H. v. (1832). *Palaeologica zur Geschichte der Erde und ihrer Geschöpfe*. S. Schmerber.

Miedema, F., Spiekman, S. N. F., Fernandez, V., Reumer, J. W. F., & Scheyer, T. M. (2020). Cranial morphology of the tanystropheid *Macrocnemus bassanii* unveiled using synchrotron microtomography. *Scientific Reports, 10*(12412), 1–19. https://doi.org/10.1038/s41598-020-68912-4

Morales, M. E., & Goloboff, P. A. (2023). New TNT routines for parallel computing with MPI. *Molecular Phylogenetics and Evolution, 178*, 107643. https://doi.org/10.1016/j.ympev.2022.107643

Müller, R. T., Ezcurra, M. D., Garcia, M. S., Agnolín, F. L., Stocker, M. R., Novas, F. E., Soares, M. B., Kellner, A. W. A., & Nesbitt, S. J. (2023). New reptile shows dinosaurs and pterosaurs evolved among diverse precursors. *Nature, 620*(7974), 589–594. https://doi.org/10.1038/s41586-023-06359-z

Nesbitt, S. J. (2011). The early evolution of archosaurs: Relationships and the origin of major clades. *Bulletin of the American Museum of Natural History, 352*, 1–292. https://doi.org/10.1206/352.1

Nesbitt, S. J., Flynn, J. J., Pritchard, A. C., Parrish, J. M., Ranivoharimanana, L., & Wyss, A. R. (2015). Postcranial anatomy and relationships of *Azendohsaurus madagaskarensis*. *Bulletin of the American Museum of Natural History, 398*, 1–126. https://doi.org/10.1206/amnb-899-00-1-126.1

Nopcsa, F. B. (1923). Neubeschreibung des Trias-Pterosauriers *Tribelesodon*. *Paläontologische Zeitschrift, 5*, 161–181. https://doi.org/10.1007/BF03160365

Nopcsa, F. B. (1928). The genera of reptiles. *Palaeobiologica, 1*, 168–188.

Nopcsa, F. B. (1931). Notizen über Macrochemus Bassanii nov. gen. et spec. *Centralblatt für Mineralogie, Geologie und Paläontologie B, 7*, 252–255.

Nosotti, S. (2007). *Tanystropheus longobardicus* (Reptilia, Protorosauria): Reinterpretations of the anatomy based on new specimens from the Middle Triassic of Besano (Lombardy, northern Italy). *Memorie Della Società Italiana Di Scienze Naturali e Del Museo Civico Di Storia Naturale Di Milano, 35*, 1–88.

O Connor, P. M. (2007). The postcranial axial skeleton of *Majungasaurus crenatissimus* (Theropoda: Abelisauridae) from the Late Cretaceous of Madagascar. *Journal of Vertebrate Paleontology, 27*(S2), 127–163. https://doi.org/10.1671/0272-4634(2007)27[127:TPASOM]2.0.CO;2

Paes-Neto, V. D., Lacerda, M. B., Ezcurra, M. D., Raugust, T., Trotteyn, M. J., Soares, M. B., Schultz, C. L., Pretto, F. A., Francischini, H., & Martinelli, A. G. (2023). New rhadinosuchine proterochampsids from the late Middle-early Late Triassic of southern Brazil enhance the diversity of archosauriforms. *The Anatomical Record*. https://doi.org/10.1002/ar.25294

Parrington, F. R. (1935). On Prolacerta broomi, gen. et sp. n. and the origin of lizards. *Annals and Magazine of Natural History Series 10, 16(92)*, 197–205. https://doi.org/10.1080/00222933508655037

Pei, R., Pittman, M., Goloboff, P. A., Dececchi, T. A., Habib, M. B., Kaye, T. G., Larsson, H. C. E., Norell, M. A., Brusatte, S. L., & Xu, X. (2020). Potential for powered flight neared by most close avialan relatives, but few crossed its thresholds. *Current Biology, 30*(20), 4033-4046. E4038. https://doi.org/10.1016/j.cub.2020.06.105

Peyer, B., & Kuhn-Schnyder, E. (1955). Squamates du Trias. In J. Piveteau (Ed.), *Traité de Paléontologie* (pp. 578–605). Masson.

Pol, D., & Escapa, I. H. (2009). Unstable taxa in cladistic analysis: Identification and the assessment of relevant characters. *Cladistics, 25*(5), 515–527. https://doi.org/10.1111/j.1096-0031.2009.00258.x

Pratt, B. R. (1998). Syneresis cracks: Subaqueous shrinkage in argillaceous sediments caused by earthquake-induced dewatering. *Sedimentary Geology, 117*(1–2), 1–10. https://doi.org/10.1016/S0037-0738(98)00023-2

Pritchard, A. C., Turner, A. H., Nesbitt, S. J., Irmis, R. B., & Smith, N. D. (2015). Late Triassic tanystropheids (Reptilia, Archosauromorpha) from Northern New Mexico (Petrified Forest Member, Chinle Formation) and the biogeography, functional morphology, and evolution of Tanystropheidae. *Journal of Vertebrate Paleontology, 35*(2), e911186. https://doi.org/10.1080/02724634.2014.911186

Puff, P., & Radzinski, K.-H. (1980). Ergebnisse und Probleme stratigraphischer Untersuchungen im mittleren Buntsandstein der DDR. *Zeitschrift Für Geologische Wissenschaften, 8*, 965–983.

Puff, P., & Radzinski, K.-H. (2013). Der Buntsandstein in der Thüringischen Senke. In J. Lepper & H.-G. Röhling (Eds.), *Stratigraphie von Deutschland XI. Buntsandstein. Schriftenreihe der Deutschen Gesellschaft für Geowissenschaften* (Vol. 69, pp. 421–448).

Renesto, S. (1994). A new prolacertiform reptile from Late Triassic of northern Italy. *Rivista Italiana Di Paleontologia e Stratigrafia, 100*(2), 285–306.

Renesto, S. (2005). A new specimen of *Tanystropheus* (Reptilia Protorosauria) from the Middle Triassic of Switzerland and the ecology of the genus. *Rivista Italiana Di Paleontologia e Stratigrafia, 111*(3), 377–394. https://doi.org/10.13130/2039-4942/6327

Renesto, S., & Saller, F. (2018). Evidences for a semi aquatic life style in the Triassic diapsid reptile *Tanystropheus*. *Rivista Italiana Di Paleontologia e Stratigrafia, 124*(1), 23–34. https://doi.org/10.13130/2039-4942/9541

Rieppel, O. (1989). The hind limb of *Macrocnemus bassanii* (Nopcsa) (Reptilia, Diapsida): Development and functional anatomy. *Journal of Vertebrate Paleontology, 9*(4), 373–387. https://doi.org/10.1080/02724634.1989.10011771

Rieppel, O. (2000). *Handbuch der Paläoherpetologie. Encyclopedia of Paleoherpetology. Part 12A. Sauropterygia I. Placodontia, Pachyleurosauria, Nothosauroidea, Pistosauroidea.* Dr. Friedrich Pfeil.

Rieppel, O., & Brinkman, P. D. (1996). *Nothosaurus* Munster, 1834 (Reptilia, Sauropterygia): Proposed precedence over *Conchiosaurus* Meyer, (1833). *Bulletin of Zoological Nomenclature, 53*(4), 270–272.

Rieppel, O., Fraser, N. C., & Nosotti, S. (2003). The monophyly of Protorosauria (Reptilia, Archosauromorpha): a preliminary analysis. *Atti Della Società Italiana Di Scienze Naturali e Del Museo Civico Di Storia Naturale Di Milano, 144*(II), 359–382.

Rieppel, O., & Wild, R. (1996). A revision of the genus *Nothosaurus* (Reptilia: Sauropterygia) from the Germanic Triassic, with comments on the status of *Conchiosaurus clavatus*. *Fieldiana Geology New Series, 34*, 1–82.

Romer, A. S. (1956). *Osteology of the reptiles*. The University of Chicago Press.

Sander, P. M., Rieppel, O. C., & Bucher, H. (1997). A new pistosaurid (Reptilia: Sauropterygia) from the Middle Triassic of Nevada and its implications for the origin of the plesiosaurs. *Journal of Vertebrate Paleontology, 17*(3), 526–533. https://doi.org/10.1080/02724634.1997.10010999

Scheyer, T. M., Wang, W., Li, C., Miedema, F., & Spiekman, S. N. F. (2020). Osteological re-description of *Macrocnemus fuyuanensis* (Archosauromorpha, Tanystropheidae) from the Middle Triassic of China. *Vertebrata PalAsiatica, 58*(3), 169–187. https://doi.org/10.19615/j.cnki.1000-3118.200525

Schmidt, M. (1928). *Die Lebewelt unserer Trias*. F. Rau.

Schoch, R. R. (2018). The temnospondyl *Parotosuchus nasutus* (v. Meyer, 1858) from the Early Triassic Middle Buntsandstein of Germany. *Palaeodiversity., 11*(1), 107–126.

Schoch, R. R. (2019). Osteology of the temnospondyl *Trematosaurus brauni* Burmeister, 1849 from the Middle Buntsandstein of Bernburg. *Germany. Palaeodiversity, 12*(1), 41–63. https://doi.org/10.18476/pale.v12.a4

Sennikov, A. G. (2011). New tanystropheids (Reptilia: Archosauromorpha) from the Triassic of Europe. *Paleontological Journal, 45*(1), 90–104. https://doi.org/10.1134/s0031030111010151

Sobral, G. (2023). The holotype of the basal archosauromorph *Prolacerta broomi* revisited. *Acta Palaeontologica Polonica, 68*(3), 393–413.

Spiekman, S. N. F., Ezcurra, M. D., Butler, R. J., Fraser, N. C., & Maidment, S. C. R. (2021a). *Pendraig milnerae*, a new small-sized coelophysoid theropod from the Late Triassic of Wales. *Royal Society Open Science, 8*(10), 210915. https://doi.org/10.1098/rsos.210915

Spiekman, S. N. F., Fraser, N. C., & Scheyer, T. M. (2021b). A new phylogenetic hypothesis of Tanystropheidae (Diapsida, Archosauromorpha) and other "protorosaurs", and its implications for the early evolution of stem archosaurs. *PeerJ, 9*, e11143. https://doi.org/10.7717/peerj.11143

Spiekman, S. N. F., & Klein, N. (2021). An enigmatic lower jaw from the lower Muschelkalk (Anisian, Middle Triassic) of Winterswijk provides insights into dental configuration, tooth replacement and histology. *Netherlands Journal of Geosciences, 100*, e17. https://doi.org/10.1017/njg.2021.12

Spiekman, S. N. F., Neenan, J. M., Fraser, N. C., Fernandez, V., Rieppel, O., Nosotti, S., & Scheyer, T. M. (2020a). Aquatic habits and niche partitioning in the extraordinarily long-necked Triassic reptile *Tanystropheus*. *Current Biology, 30*, 1–7. https://doi.org/10.1016/j.cub.2020.07.025

Spiekman, S. N. F., Neenan, J. M., Fraser, N. C., Fernandez, V., Rieppel, O., Nosotti, S., & Scheyer, T. M. (2020b). The cranial morphology of *Tanystropheus hydroides* (Tanystropheidae, Archosauromorpha) as revealed by synchrotron microtomography. *PeerJ, 8*, e10299. https://doi.org/10.7717/peerj.10299

Spiekman, S. N. F., & Scheyer, T. M. (2019). A taxonomic revision of the genus *Tanystropheus* (Archosauromorpha, Tanystropheidae). *Palaeontologia Electronica, 22*(3), 1–46. https://doi.org/10.26879/1038

Spiekman, S. N. F., Wang, W., Lijun, Z., Rieppel, O., Fraser, N. C., & Chun, L. (2024). *Dinocephalosaurus orientalis* Li, 2003: a remarkable marine archosauromorph from the Middle Triassic of southwestern China. *Earth and Environmental Science Transactions of the Royal Society of Edinburgh*, 1–33. https://doi.org/10.1017/S175569102400001X

Tschanz, K. (1986). Funktionelle Anatomie der Halswirbelsäule von *Tanystropheus longobardicus* (Bassani) aus der Trias (Anis/Ladin) des Monte San Giorgio (Tessin) auf der Basis vergleichend morphologischer Untersuchungen an der Halsmuskulatur rezenter Echsen. *PhD thesis Universität Zürich*.

Tschanz, K. (1988). Allometry and heterochrony in the growth of the neck of Triassic prolacertiform reptiles. *Palaeontology, 31*(4), 997–1011.

Vaughn, P. (1955). The Permian reptile *Araeoscelis* restudied. *Bulletin of the Museum of Comperative Zoology, 113*(5), 305–467.

Wang, W., Lei, H., & Li, C. (2023a). A small-sized dinocephalosaurid archosauromorph from the Middle Triassic of Yunnan, southwestern China. *Vertebrata PalAsiatica*. https://doi.org/10.19615/j.cnki.2096-9899.231013

Wang, W., Spiekman, S. N., Zhao, L., Rieppel, O., Scheyer, T. M., Fraser, N. C., & Li, C. (2023b). A new long-necked archosauromorph from the Guanling Formation (Anisian, Middle Triassic) of southwestern China and its implications for neck evolution in tanystropheids. *The Anatomical Record*. https://doi.org/10.1002/ar.25216

Wang, Y., Yang, D., Han, J., Wang, L., Yao, J., & Liu, D. (2014). The Triassic U-Pb age for the aquatic long-necked protorosaur of Guizhou. *China. Geological Magazine, 151*(4), 749–754. https://doi.org/10.1017/S001675681400003X

Watson, D. M. S. (1912). Mesosuchus browni, gen. et spec. nov. *Records of the Albany Museum*, *2*, 298–299.

Watson, D. M. S. (1951). *Paleontology and modern biology*. Oxford University Press.

Watson, D. M. S. (1957). On *Millerosaurus* and the early history of the sauropsid reptiles. *Philosophical Transactions of the Royal Society of London. Series b, Biological Sciences, 240*(673), 325–398.

Wedel, M., & Taylor, M. (2023). The biomechanical significance of bifurcated cervical ribs in apatosaurine sauropods. *Vertebrate Anatomy Morphology Palaeontology, 11*, 91–100.

Weigelt, J. (1989). *Recent vertebrate carcasses and their paleobiological implications*. University of Chicago Press.

Wild, R. (1973). Die Triasfauna der Tessiner Kalkalpen XXII. *Tanystropheus longobardicus* (Bassani) (Neue Ergebnisse). *Schweizerische Paläontologische Abhandlungen, 95*, 1–162.

Wild, R. (1980). Neue Funde von *Tanystropheus* (Reptilia, Squamata). *Schweizerische Paläontologische Abhandlungen, 102*, 1–43.

Xu, X., Wang, K., Zhao, X., Sullivan, C., & Chen, S. (2010). A new leptoceratopsid (Ornithischia: Ceratopsia) from the Upper Cretaceous of Shandong, China and its implications for neoceratopsian evolution. *PLoS ONE, 5*, e13835.

von Zittel, K. A. (1932). *Text-book of paleontology* (Vol. II). Macmillan and Co.

Publisher's Note